PRESSURE DEPENDENT EXTRINSIC EFFECTS IN InSb

by

© IAN BOOTH

A Thesis Submitted in Partial Fulfillment of the Requirements for the

DEGREE OF MASTER OF SCIENCE

DEPARTMENT OF PHYSICS
LAKEHEAD UNIVERSITY
THUNDER BAY, ONTARIO, CANADA
MAY, 1980

ACKNOWLEDGEMENTS

It gives me great pleasure to thank my research supervisor, Dr. W.J. Keeler, for his assistance and instruction throughout this work.

Special thanks are due to Professor M. Hawton for her interest in the project.

I wish to express my appreciation to Mr. G.C. Anderson for machining the pressure vessel, and helping to maintain the cryostat.

The assistance of my parents in computer analysis, which was invaluable in the theoretical analysis, is greatly appreciated.

Finally, I wish to thank Mrs. J. Boucher for typing and helping to correct the thesis.

TABLE OF CONTENTS

LIST OF FIGURES

ABSTRACT

Electrical transport properties of n and p-type InSb in the temperature range 6.2-300K have been studied under pressures up to 15 kbar using Hall measurements.

The donor gap in n-InSb is found to increase linearly with pressure, becoming zero at pressures of 8.4 kbar or less. This is responsible for carrier freeze-out under pressure. Unexpected behaviour is observed in the donor gap, as it appears to decrease abruptly at temperatures near 100K as temperature is lowered. This effect has been investigated and two possible theories explaining it are examined. Mobility measurements at low pressure indicate that at temperatures below 40K scattering processes are dominated by ionized and neutral impurity scattering. At pressures high enough to cause carrier freeze-out the mobility decreases rapidly with temperature. High electric field measurements indicate that ionized impurity scattering is the dominant scattering mechanism in this regime.

PRESSURE DEPENDENT EXTRINSIC EFFECTS IN InSb

A member of the III-V family of semiconductors, InSb was for many years considered a classic example of a narrow band-gap semiconductor. Recently there has been renewed interest in the donor states of this material, of which there is a surprisingly limited understanding.

The effect of donor freeze-out observed in many semiconductors is not seen in InSb at any temperature without the action of a magnetic field, pressure or some other agent. The explanation of this seems to be that the low electron effective mass 0.013 m_e in InSb results in large donor orbits which overlap for even the purest samples available (about 10^{13} donors/cc) causing the donor level to spread and overlap with the conduction band.

Magnetically induced freeze-out has been studied fairly extensively by various workers.[1-9] Two theories of magnetic freeze-out are prevalent. One is that the donor levels are initially in the conduction band or very near to it, and that a magnetic field raises the conduction band minimum more than it does the donor level relative to the valence band, thus increasing the donor gap.[2,3,4] Alternatively, the donor electron wavefunctions may overlap sufficiently to form a donor band which causes conduction at low temperature.[1,6] The magnetic field compresses the donor electron

wavefunctions so that impurity band conduction is destroyed and freeze-out is observed.

The effect of pressure induced donor freeze-out is not as well understood as magnetic freeze-out, and less experimental work has been done on it. Apart from some combined pressure and magnetic field investigations,[10,11] the primary researchers in the field are Porowski and his co-workers.[12-15] They have observed strongly pressure dependent donor freeze-out in n-type InSb, as well as an anomalous effect during freeze-out which appears to be a sudden change of the donor gap at about 100^{o}K. This they explain in terms of a donor atom that can occupy non-equivalent lattice positions with different electron energies.

Studies of acceptor levels in InSb are rare, and an understanding of them could be helpful in elucidating some effects in n-InSb. Because electrons in InSb are much lighter than holes their mobility is much higher (about 80 times), consequently, in order to appear p-type the material must be doped with enough acceptors to override the effect of donor electrons, so p-type InSb cannot be as pure as n-InSb.

The effect of a high electric field on mobility and carrier number in semiconductors has been investigated experimentally[16,17] and theoretically.[18,19] The electron mobility in InSb has been given a theoretical treatment in some detail by T. Stokoe and J. Cornwell.[19] Their low temperature results will be compared

with our experimental data in the freeze-out range. Impact ionization of donors in InSb does not seem to have received as much theoretical attention, although some experimenters have observed it during freeze-out experiments.[1,2,11] Measurement of breakdown voltages for donor impact ionization can reveal the presence of more than one donor level by the existence of more than one breakdown voltage. In cases of extreme freeze-out the measuring fields used could cause impact ionization and affect the results, so it is important to know when this becomes significant.

Optical measurements on semiconductors can provide information on energy gaps more directly than electrical measurements. Anomalous optical absorption in pure and doped samples of InSb have been observed by M. Tanenbaum and H.B. Briggs,[20] and by Elias Burstein[21] who explains the effect in terms of degeneracy of conduction band electrons for high electron density. We have observed degeneracy effects in our samples at low temperatures and low pressure.

We have studied the Hall effect and resistivity for n and p-type InSb between room temperature and $7^{o}K$ at pressures up to 15 kbar. This thesis studies the Porowski anomaly, and considers alternative explanations. Freeze-out in p-type material is examined to see if a similar effect occurs there. Electron number and mobility in the freeze-out range are measured for

varying electric and magnetic fields and the results compared with theory.

In Chapter 1 the theory of low field carrier number under extrinsic conditions is reviewed and the effects of various doping conditions is considered. Low and high field mobility are discussed and the current theories of magnetic freeze-out briefly presented. The van der Pauw method used for measurements is examined. In Chapter 2 the sample preparation and equipment are described. In Chapter 3 the results are presented and discussed, and Chapter 4 contains our conclusions.

Chapter 1

Theoretical Considerations

1-1. Band Structure in InSb

There is a reasonable amount of information on the band structure of InSb.

The maxima and minima of the valence and conduction band respectively lie around $\vec{k} = 0$. The conduction band is made up of two bands, the lowest of which lies at the centre of the Brillouin zone (Γ point) where the band has the largest curvature, hence the smallest electron effective mass. The band is approximately parabolic for energies up to a few tens of millelectron volts at zero pressure, and the parabolic approximation becomes better as pressure increases the band gap. The band structure of InSb is shown graphically in Figure I.

Kane[22] has performed detailed calculations of the band structure of InSb and other small band gap semiconductors. He obtains the $E - \vec{k}$ relations for the conduction and valence bands using p, the interband interaction matrix element and Δ, the spin-orbit splitting energy at $\vec{k} = 0$. For the conduction band (energy measured from the top of the valence band)

$$E = E_g + \frac{\hbar^2 k^2}{2m_o} + \frac{1}{2}\left[\left(E_g^2 + \frac{8p^2k^2}{3}\right)^{\frac{1}{2}} - E_g\right].$$

Figure 1 Band structure of InSb. The dashed lines represent the bands under a pressure of approximately 15 kbar.

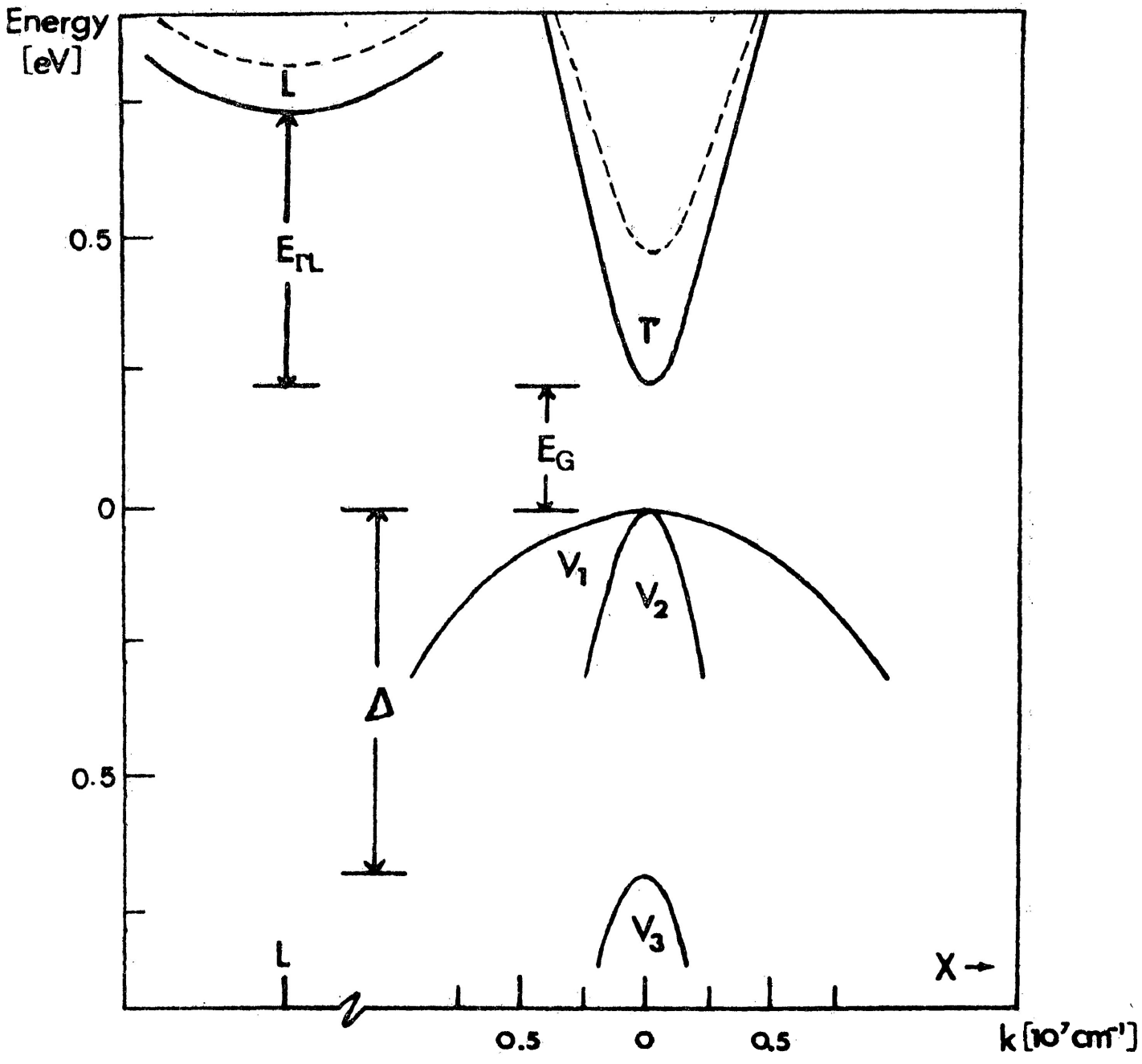
Energy
[eV]
L
$E_{\Gamma L}$
Γ
E_G
0.5
0
0.5
V_1
V_2
Δ
V_3
L
X
0.5
0
0.5
k [10⁷cm⁻¹]

For the valence bands (energy measured from the top of the valence band)

$$E = -\frac{\hbar^2 k^2}{2m_o} \qquad \text{Heavy hole band}$$

$$E = -\frac{\hbar^2 k^2}{2m_o} - \frac{1}{2}\left[\left(E_g^2 - \frac{8p^2k^2}{3}\right)^{\frac{1}{2}} - E_g\right] \qquad \text{Light hole band}$$

$$E = -\Delta - \frac{\hbar^2 k^2}{2m_o} - \frac{p^2k^2}{3(E_g+\Delta)} \qquad \text{Spin-orbit split band.}$$

Here m_o is the free electron mass and E_g is the valence to conduction band gap. The parameter Δ occurs only in the spin-orbit split band expression.

In the conduction band formula, if we measure energy from the bottom of the conduction band and ignore $\hbar^2k^2/2m_o$ (since $m_o \simeq 80m_n^*$ in the conduction band), we have

$$E' = \frac{1}{2}\left[\left(E_g^2 + \frac{8p^2k^2}{3}\right)^{\frac{1}{2}} - E_g\right] . \qquad (1\text{-}1\text{-}1)$$

We define $m_n^* = 3\hbar^2E_g/4p^2$. Putting this in (1-1-1) and eliminating p^2, one obtains

$$\frac{\hbar^2k^2}{2m_n^*} = E'\left(1 + E'/E_g\right) \qquad (1\text{-}1\text{-}2)$$

This is a hyperbolic relation between E' and $\vec{k}$. Provided the conduction band is not too full and the electron energies are not too high ($E' << E_g$) the equation reduces to a parabolic relation between E' and $\vec{k}$:

$$E' = \hbar^2 k^2 / 2m_n^* \qquad (1\text{-}1\text{-}3)$$

The effect of pressure is to increase E_g and m_n^*. Thus the parabolic approximation is improved both directly by reduction of E'/E_g and by the larger density of states, which is proportional to $m_n^{*3/2}$.

The L conduction band edge is estimated to lie 0.52 eV above the Γ conduction band minimum. The pressure derivatives of the Γ and L band minima are estimated to be 14×10^{-3} eV/kbar and 8.3×10^{-3} eV/kbar respectively.[23,24,25]

The valence bands V_1 and V_2 are degenerate at $\vec{k} = 0$. The hole density of states is determined mainly by the low-curvature heavy hole band, however, the electrical properties are affected by both types of holes since the light holes are more mobile than the heavy holes. The split off band V_3 does not contribute in low electric field studies.

1-2. Low Field Carrier Concentration for Extrinsic Semiconductors

The electron density in the conduction band for a semiconductor with parabolic bands is given by

$$n = N_c F_{1/2}(\eta) \tag{1-2-1}$$

where $$F_{1/2}(\eta) = \frac{2}{\sqrt{\pi}} \int \frac{\sqrt{\varepsilon}\, d\varepsilon}{1+\exp(\varepsilon-\eta)} \tag{1-2-2}$$

$$\varepsilon = \frac{E-E_c}{kT} \qquad \eta = \frac{\phi-E_c}{kT} \qquad \phi = \text{Fermi energy.}$$

$N_c = 2(2\pi m_e^* kT/h^2)^{3/2}$ is the effective density of states in the conduction band, m_e^* is the electron effective mass.

If there is a concentration of donor atoms N_d with ionization energy E_d, the number of deionized donors will be

$$N_{dn} = \frac{N_d}{1+B\exp\left(\frac{E_c-\phi-E_d}{kT}\right)} \tag{1-2-3}$$

But $$N_d^+ = N_d - N_{dn} . \tag{1-2-4}$$

N_d^+ is the number of ionized donors.

For the non-degenerate case where $E_c - \phi \geq 4kT$ we have

$$n = N_c F_{1/2}(n) \simeq N_c \exp(n) = N_c \exp\left(\frac{\phi - E_c}{kT}\right) \tag{1-2-5}$$

Substituting (1-2-3) and (1-2-5) in (1-2-4) we obtain

$$N_d^+ = \frac{N_d}{1+\mathcal{B}^{-1}\exp\left(\frac{E_d+\phi-E_c}{kT}\right)} = \frac{N_d}{1+\frac{n}{\mathcal{B}N_c}\exp\left(\frac{E_d}{kT}\right)} \tag{1-2-6}$$

A similar expression exists for the number of ionized acceptors. That is

$$N_A^- = \frac{N_A}{\frac{p}{\mathcal{B}N_V}\exp\left(\frac{E_A}{kT}\right)+1} \tag{1-2-7}$$

where $N_V = 2(2\pi k_B T m_p^*/h^2)^{3/2}$ is the density of hole states in the valence band and $\mathcal{B}$ is a factor that accounts for possible multiplicity in atom bound states. This will be taken as 2.

To solve for the carrier concentration in the conduction band, two other equations are required. From charge neutrality

$$P + N_D^+ = n + N_A^- \tag{1-2-8}$$

and the intrinsic carrier concentration of carriers excited across the valence to conduction band gap gives

$$n_p = N_c N_V \exp\left(\frac{-E_G}{k_B T}\right) \qquad (1\text{-}2\text{-}9)$$

where E_G is the valence to conduction band gap.

The four equations (1-2-6) to (1-2-9) can be solved to find the free electron or hole concentration for any ratio of N_A and N_D. However, this would involve solving a fourth order equation, so it is helpful to consider simpler cases.

If there are no compensating acceptors, the free electron concentration is simply

$$n = N_D^+ = \frac{N_D}{1 + \frac{n}{BN_c} \exp\left(\frac{E_D}{k_B T}\right)}$$

or

$$\frac{n^2}{N_D - n} = BN_c \exp\left(\frac{-E_D}{k_B T}\right) \qquad (1\text{-}2\text{-}10)$$

In the case of a lightly compensated sample $N_D >> N_A$ we can make the approximation (in the extrinsic range)

$$N_D^+ \simeq n + N_A \qquad (1\text{-}2\text{-}11)$$

because all the acceptors will have electrons frozen onto them. Putting this in (1-2-6) we have

$$\frac{n(n+N_A)}{N_D-N_A-n} = \mathcal{B}N_C \exp\left(\frac{-E_D}{k_B T}\right) \qquad (1\text{-}2\text{-}12)$$

This equation can give anomolous appearances. For moderate freeze-out $N_D >> n >> N_A$,

$$\frac{n(N_A+n)}{N_D-N_A-n} \simeq \frac{n^2}{N_D} .$$

Therefore

$$n = \sqrt{N_C N_D \mathcal{B}} \quad \exp\left(\frac{-E_D}{2k_B T}\right) \qquad (1\text{-}2\text{-}13)$$

But for extreme freeze-out $N_D >> N_A >> n$,

$$\frac{n(N_A+n)}{N_D-n-N_A} \simeq \frac{nN_A}{N_D}$$

and

$$n = \mathcal{B}N_C N_D/N_A \exp\left(\frac{-E_D}{k_B T}\right) . \qquad (1\text{-}2\text{-}14)$$

Thus the energy gap appears to double as the number of carriers decreases past $n = N_A$. A plot of log $(n/T^{3/2})$ against $1/T$ will show

two straight lines with one having twice the slope of the other intersecting at $n = N_A$. This has been observed experimentally and may be used to obtain information about compensation levels in a semiconductor.

For heavily compensated semiconductors the solution must be obtained by solving the four equations (1-2-6) to (1-2-9) giving

$$\frac{N_C N_V}{n} \exp(-\varepsilon_G) + \frac{N_D N_C}{2n\exp(\varepsilon_D)+N_C} = n + \frac{nN_A}{2N_C\exp(\varepsilon_A-\varepsilon_G)+n} \qquad (1\text{-}2\text{-}15)$$

where $\varepsilon_D = E_D/k_BT$ $\varepsilon_A = E_A/k_BT$ $\varepsilon_G = E_G/k_BT$ and we have assumed twofold degeneracy for both donors and acceptors.

This equation gives the carrier number under all conditions of doping and compensation.

Equations of this type can best be solved by numerical methods. This will be discussed further in section 1-5, part III.

1-3. Low and High Field Mobility

The mobility of carriers in a crystal is limited by several processes whose effects are generally dependent on lattice temperature, carrier temperature, carrier effective mass, and ionization conditions. The most important scattering mechanisms in InSb at temperatures below $\sim 50^{o}K$ are ionized and neutral impurity scattering. At high temperature, phonon and electron hole scattering predominate. The low field mobility limits for these processes have been given in a previous thesis by S.M. Fong.[26] The impurity scattering formulas are of interest to us as we are concerned with mobilities at low temperatures, however, the high field behaviour of phonon scattering is also considered as it could play a role when the carrier temperature becomes elevated.

I. Ionized Impurity Scattering

At low temperatures, when phonon scattering becomes less effective, the mobility limit may be controlled by ionized impurity scattering. The mobility limit has been given as[27]

$$\mu_I = 3.2\times10^{15}\left(\frac{m_o}{m^*}\right)^{\frac{1}{2}} \frac{k^2 T^{3/2}}{N_D+N_A} \Big/ \ell n \left[1.3\times10^{14} T^2 k \left(\frac{m^*}{m_o}\right) \Big/ n \right]. \quad (1\text{-}3\text{-}1)$$

N_D and N_A are the number of ionized donors and acceptors, n is the free carrier concentration, and k is the dielectric constant of the material.

The units used are in the cgs system. The mobility will be in the $cm^2/V\text{-}sec$. We have for low fields

$$\mu_I \alpha (m^*)^{-\frac{1}{2}} T^{3/2}$$

The scattering time τ giving the effective collision period is related to carrier energy by[28]

$$\tau \alpha E^{3/2} . \qquad (1\text{-}3\text{-}2)$$

Similarly, the Hall factor is

$$Y_H = 315\pi/512.$$

The ionized impurity mobility limit is observed to drop rapidly when an electric field raises the electron energy. Since the scattering time is proportional to $E^{3/2}$, an increase in the electron's energy by the field will result in its being scattered less so that it can increase its energy still further. The mobility will undergo a runaway increase for a small range of field strengths until it is limited by some other process. When freeze-out of donors is advanced, the number of ionized impurities will be reduced. The application of a high electric field may cause impact ionization, increasing the ionized impurity concentration, and reducing the mobility limit due to this process. Thus the field dependence of ionized impurity scattering in a sample exhibiting extreme freeze-out will be the difference of these two competing processes.

II. Neutral Impurity Scattering

Scattering by neutral impurities may be of importance in samples experiencing a high degree of freeze-out. Erginsoy[29] has given a simple treatment of this process for low temperatures.

$$\mu_N = 1.4 \times 10^{22} \left(\frac{m^*}{m_o}\right) \frac{1}{kN_N} \quad cm^2/V\text{-}sec. \tag{1-3-3}$$

N_N = number of neutral impurities per cc.

Again we have[28]

$$\mu_n \alpha m^* T^o \quad \text{and} \quad \tau \alpha E^o \tag{1-3-4}$$

Here the Hall factor is $Y_H = 1$

Because the scattering time is independent of the carrier energy, the mobility limit has no explicit temperature or field dependence. Since the number of neutral impurities is temperature dependent and may also be reduced by impact ionization, the neutral impurity scattering process is indirectly affected by these parameters, and will generally become less effective when temperature or electric field strength is raised.

III. Phonon Scattering

Carriers may be scattered by lattice vibrations or phonons. Acoustic phonons are present in all types of lattice, while polar optical phonons occur only in diatomic lattices since they rely on the relative movement of two unlike atoms. The low field mobility limits for optical and acoustic phonon scattering are given in the thesis of S.M. Fong, however, they are of little concern here because phonon scattering, since it relies on thermal lattice vibrations, becomes insignificant at low temperatures. When the electron energy is raised by an electric field it may dissipate some of this energy in the form of acoustic or optical phonons. Thus, the high field mobility limits of these processes may be of importance.

A theoretical treatment of high field acoustic and polar optical scattering is given by Seeger.[30] The mobility limit due to acoustic phonons at high field exhibits a characteristic $E^{-\frac{1}{2}}$ field dependence

$$\frac{\mu}{\mu_o} = 1.81 \left(\frac{u_1}{\mu_o}\right)^{\frac{1}{2}} E^{-\frac{1}{2}} \qquad (1\text{-}3\text{-}4)$$

where μ_o is the low field mobility, and u_1 is the speed of sound in the material.

This result is verified by experimental observations of the field dependent mobility in germanium.[17]

Polar optical scattering is also effective in InSb since it is a diatomic material. The mobility limit due to this process exhibits a runaway increase at sufficiently high field strengths, an effect that has been related to dielectric breakdown. It has never been observed in a semiconductor because other scattering mechanisms take over at high enough fields. D. Matz has pointed out that the non-parabolic conduction band in InSb would prevent the breakdown.[18]

At low lattice temperatures ($T << \theta$, where θ is the Debye temperature) the drift velocity may be limited to a nearly constant value over a range of field strengths before the breakdown. This would result in a mobility field dependence of approximately E^{-1} .

IV. Combined Scattering Processes

E.M. Conwell[17] has measured the electron mobility in germanium at $20^{o}K$, and observes that it rises rapidly for a small range of electric fields and then decreases as $E^{-\frac{1}{2}}$. For higher temperatures the mobility is constant with field up to some point and then decreases as $E^{-\frac{1}{2}}$ at high fields. She attributes this behaviour to a combination of ionized impurity and acoustic scattering. The ionized impurity scattering limits the mobility at $20^{o}K$

and its effect decreases rapidly with increasing field until acoustic scattering takes over with its characteristic $E^{-\frac{1}{2}}$ mobility dependence. At higher temperatures ($77^{o}K$) acoustic scattering is dominant at all electric field strengths.

In InSb, however, polar optical scattering may play an important role since we are dealing with a diatomic material. T.Y. Stokoe and J.F. Cornwell[19] have analyzed high field transport in n-InSb using the drifted Maxwellian approach, taking the dielectric constant as 17.5 and the acoustic deformation potential as -7.2 eV. They take into account in their calculations mixing of Bloch states, spin reversal scattering, and band non-parabolicity.

For a lattice temperature of $77^{o}K$ they calculate that polar scattering is the dominant process for electron temperatures up to $400^{o}K$ or more.

They also calculate the field dependence of the mobility for lattice temperatures of $20^{o}K$, taking into account band non-parabolicity, Bloch state mixing, polar, acoustic and ionized impurity scattering. The results give a field dependence for low fields ($E \leq 10V/cm$) of $\mu \alpha E^{0.25}$ and for high fields ($E \geq 30V/cm$) $\mu \alpha E^{-0.77}$. These results will be compared with some of our experimental work which was also done near $20^{o}K$.

V. Impact Ionization

At low temperatures and high enough pressures most of the electrons in n-InSb freeze out onto donors. As the electric

field across the sample is increased, some of the free electrons acquire sufficient energy to ionize these neutral donor atoms. For donor levels of the order of 10 meV below the conduction band, impact ionization begins to increase the number of electrons for fields of about 0.1 V/cm. The increase in carrier number with field should be exponential[31] and the power of the exponential is proportional to the mobility, i.e.

$$g(E) \alpha \exp(\mu E)$$

The rate of impact ionization can also be affected by a magnetic field. Z. Dobrovolskis and A. Krotkus[32] observed an increase in ionization for small magnetic fields, while larger fields retarded the ionization.

They explain this by magnetic cooling of the electrons at high magnetic fields, while at low fields (670 Oe) the main effect of the magnetism is to cause distortions in current paths, resulting in inhomogeneous electric fields in the sample and areas of high local ionization. They observe the carrier generation rate to be exponential with electric field strength.

If the electric field is increased sufficiently the ionization rate will enter a region of breakdown where the number of carriers increases very rapidly with field until all the donors are ionized, when the carrier number will become constant. If

more than one donor level is present a distinct breakdown should be observed for each level. An example is zinc doped germanium (two acceptor levels: E_{A_1} = 33 meV, E_{A_2} = 90 meV) which exhibits two regions of breakdown in an n vs. $\vec{E}$ plot.

1-4. Hall Effect Measurement and the Van der Pauw Technique

Van der Pauw[33] has developed a method of measuring the specific resistivity and Hall resistivity of flat samples of arbitrary shape. This method holds if the following conditions are met:

(a) The contacts are at the circumference of the sample.

(b) The contacts are sufficiently small.

(c) The sample is of uniform thickness.

(d) The sample has no isolated holes.

The specific resistivity is given by

$$p = \frac{\pi d}{2\ell n 2} \left(R_{AB,CD} + R_{BC,DA}\right) f\left(\frac{R_{AB,CD}}{R_{BC,DA}}\right) \qquad (1\text{-}4\text{-}1)$$

where d is the sample thickness, $R_{AB,CD}$ is the resistance defined as the voltage between D and C per unit current between A and B contacts. The resistance $R_{BC,DA}$ is defined in a similar manner.

The parameter f is a slowly varying function of the ratio $R_{AB,CD}/R_{BC,DA}$. Van der Pauw gives the relation satisfied by f as

$$\frac{R_{AB,CD} - R_{BC,AD}}{R_{AB,CD} - R_{BC,AD}} = f \text{ arc cosh } \left\{\frac{\exp(\ell n(2)/f)}{2}\right\} \qquad (1\text{-}4\text{-}2)$$

This equation is consistent with Van der Pauw's graph of f against $(R_{AB,CD}/R_{BC,DA})$.

The arrangement for measurement of specific resistivity is shown in Fig. 2.

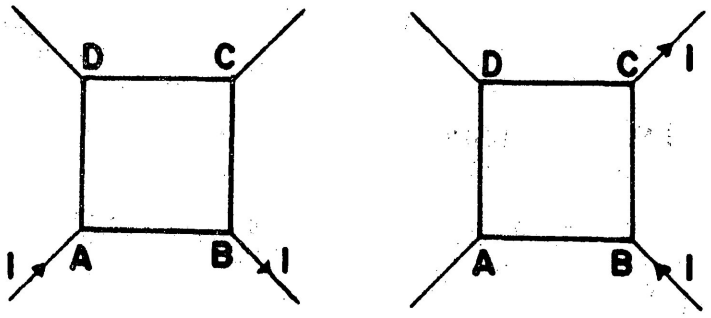

Figure 2

The Hall coefficient R_H can be determined by measuring the change of resistivity $\Delta R_{BD,AC}$ when a magnetic field $\vec{B}$ is applied perpendicular to the sample. We have

$$R_H = \frac{d}{|\vec{B}|} \Delta R_{BD,CA} \qquad (1\text{-}4\text{-}3)$$

For n-type InSb the electron mobility is of the order of one hundred times greater than hole mobility and since the number of electrons is always equal to or greater than the number of holes the electrons dominate conduction processes and one may assume single band conduction. Then

$$R_H = \frac{d}{|\vec{B}|} R_{BD,CA} = \frac{Y_H}{ne} = \frac{1}{n_{eff}e} \qquad (1\text{-}4\text{-}4)$$

where $Y_H = \langle\mu_n^2\rangle/\langle\mu_n\rangle^2$. The Hall factor Y_H varies from 1 to 2 depending on the scattering processes. If Y_H is unknown one may obtain the Hall mobility and effective carrier number leaving Y_H undetermined.

$$\mu_H = R_H/\rho = \left(\frac{Y_H}{ne}\right) (ne\ \mu_{on}) = Y_H\ \mu_D$$

$$(\mu_{on} = \mu_n,\ \vec{B} = 0) \quad . \qquad (1\text{-}4\text{-}5)$$

One must know Y_H in order to specify the drift mobility.

The apparent carrier concentration is plotted as n throughout this thesis and is given by

$$n_{eff} = |\vec{B}|/de \frac{1}{\Delta R_{BD,CA}} = n/Y_H \qquad (1\text{-}4\text{-}6)$$

For the purpose of obtaining the derivatives of n and μ with temperature, pressure, or other parameters, there is negligible error in plotting n_{eff} and μ_H instead of n and μ_D since Y_H will only vary slowly and over a small range.

The situation is more complex in p-type InSb. At room temperature the material is intrinsic and the more mobile electrons dominate all conduction processes. As the temperature is lowered the situation changes from intrinsic to extrinsic as the proportion of electrons to holes becomes smaller. The Hall resistivity in this case is

$$R_H = \frac{Y_H}{e} \frac{p-nb^2}{(p+nb)^2} \qquad (1\text{-}4\text{-}7)$$

where $b = \mu_n/\mu_p$ and p is the number of holes. The Hall resistivity changes sign at $p = nb^2$ rather than at the intrinsic concentration $n = p$. In InSb we have $b \simeq 80$ at room temperature so the hole concentration must exceed the electron concentration by a factor of 6400 for the R_H to change sign.

In this thesis we are primarily interested in the extrinsic behaviour of InSb, which in p-type material means that the condition $p >> nb^2$ must be satisfied. In order to calculate how far below the sign change of R_H the temperature must be for extrinsic conditions to prevail we use the formula

$$np = N_C N_V \exp(-E_G/k_B T) \qquad (1\text{-}2\text{-}9)$$

E_G being the band gap energy. At the sign change we have $p \simeq 6400\ n$ which means that the concentration of holes is extrinsic, i.e. equal to the number of uncompensated acceptors.

$$p = N_A = \text{constant}$$

$$\therefore \quad n = (N_C N_V / N_A) \exp(-E_G/k_B T)$$

We know that $N_C N_V$ has a T^3 dependence, and the smallest value of E_G is at zero pressure and is about 0.2 eV. The sign change occurs at around $T = 150^{o}K$.

$$\therefore \quad n_c \propto T^3 \exp(-2321/T) = 150^3 \exp\left(\frac{-2321}{150}\right) = 6.43 \times 10^{-1} .$$

To ensure extrinsic conditions we specify $n \leq n_c/10$ which is satisfied for $T \leq 133^{o}K$. Thus it is safe to ignore electron conductivity at temperatures twenty degrees or more below the sign change in R_H .

Another complication arises in extrinsic p-type InSb, this being the two valence bands contributing heavy and light holes, with different mobilities. A simplified expression valid at low fields is

$$R_H = \frac{\gamma_H}{e} \frac{\mu_1^2 p_1 + \mu_2^2 p_2}{(\mu_1 p_1 + \mu_2 p_2)^2} \qquad (1\text{-}4\text{-}8)$$

where p_1 and p_2 are the concentrations of the two hole types, and μ_1 and μ_2 are their respective mobilities.

If the ratios $p_1/p_2 = x$ and $\mu_1/\mu_2 = b$ are known to be constant with temperature then we may solve for p_1 or p_2 :

$$R_H = \frac{1}{p_2}\left[\frac{\gamma_H}{e} \frac{b^2 x + 1}{(bx + 1)^2}\right] \qquad (1\text{-}4\text{-}9)$$

Figure 3 shows the arrangement for Hall measurements.

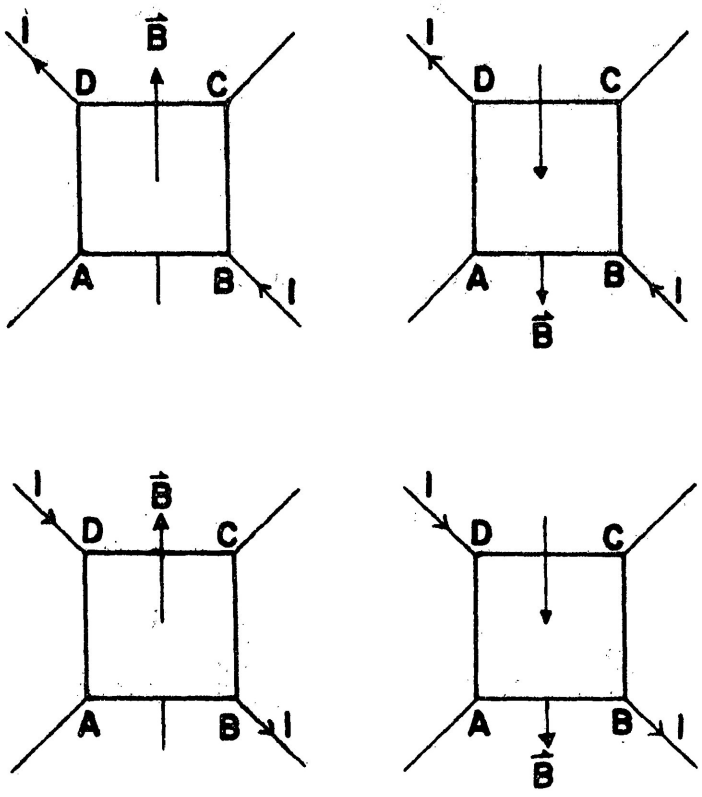

Figure 3

1-5. Donor Freeze-out in InSb

I. Magnetic Freeze-out

At zero pressure and magnetic field strength the effect of donor freeze-out is not observed in InSb at any temperature. An apparent increase in R_H at temperatures of the order of 10^oK can be attributed to the onset of degeneracy of electrons in the conduction band. Freeze-out at low temperatures has been observed when a strong magnetic field is present, and there are two distinct schools of thought as to the cause of this. R.J. Sladek[1] has made a detailed study of magnetic field effects on donor levels in InSb. He concludes that the donor levels overlap the conduction band at zero field strength, due to the low electron effective mass which causes the donor electron wavefunctions to overlap each other at even the lowest available impurity concentrations. A simple hydrogen atom model for donors in InSb gives an ionization energy of 0.69 meV but as Keys and Sladek[34] point out the average distance between donors is only about three times the reduced Bohr radius for 2×10^{14} impurities per cubic centimeter. A magnetic field would narrow the spread-out donor levels into a donor band which would lie below the conduction band. The effect of the field on conduction band electrons would be to raise their energy by $\frac{1}{2} \hbar\omega$, where ω is the cyclotron angular frequency eB/m_n^* The energy of the donor states would also be raised due to the compression of the donor electron wavefunctions closer to their atoms, but the increase would

not be as great as for conduction band electrons, thus the donor gap would increase with increasing magnetic field strength, producing freeze-out. They have observed freeze-out at temperatures in the range of 1-10^{o}K and magnetic fields up to 30 kG. The binding energy of the donors appears to increase with field as predicted, and an impurity band becomes evident at low temperature as R_H passes through a maximum and starts to decrease.

Another effect that may be responsible is the Mott transition. Fenton and Haering[4] have analyzed this in semiconductors, in particular InSb. The theory takes into account donor screening by conduction band electrons. For shallow donor states the number of electrons ionized into the conduction band could be sufficient to reduce the donor binding energy to zero by screening, thus there will be no bound states and no freeze-out. A magnetic field increases the donor gap in the manner described previously, and for some critical value of field the donor binding energy would become finite. As electrons start to freeze-out the screening decreases, so that the process is regenerative and a rapid decrease in the conduction band electron density would be observed. At absolute zero the change would become a discontinuity called a Mott transition. The field strength required to produce this obviously depends on impurity concentration since a greater number of impurities produces more screening, requiring a higher field strength to produce a transition.

M. von Orthenberg[7] has considered the problem of magnetic freeze-out theoretically, calculating the energy levels of a screened hydrogen-like impurity centre, including screening, non-parabolicity, and excited bound states. His results show good agreement with experiment in the high magnetic field range.

II. Pressure Induced Freeze-out: Porowski's Model

S. Porowski and various co-workers first observed an anomaly in donor freeze-out in undoped InSb[12,13]. The transition occurs during temperature varying, constant pressure runs when the pressure is high enough to cause freeze-out. It has the appearance of an abrupt change in the freeze-out rate (decrease) at about 100^{o}K as the temperature is lowered. Porowski and his colleagues analyzed the apparent donor gap on both sides of the transition using the donor energy gap formula

$$E_i = E_{oi} + Y_i P \qquad (1\text{-}5\text{-}1)$$

With E_i as the donor energy gap at pressure P, E_1 is the gap above 100^{o}K and E_2 the gap below 100^{o}K. Fitting his data Porowski obtains

$$E_{o1} = +85 \text{ meV} \quad Y_1 = -10.5 \text{ meV/kbar}$$
$$E_{o2} = +145 \text{ meV} \quad Y_2 = -20.0 \text{ meV/kbar}.$$

Energies are measured from the bottom of the conduction band. The pressure dependences of the donor levels Y_1 and Y_2 were seen to be close to the pressure dependence of the L and X minima respectively; it was initially assumed that the donor levels were associated with these minima. This simple model failed to explain why level 1 was not being populated above $100^{o}K$ or why level 2 was not populated below it.

Porowski ruled out any purely electronic model for the transition because the involved electrostatic potentials should lower the mobility during freeze-out, which is the opposite of what he observed. He assumes a model in which the donor atoms can occupy two or more positions in the lattice with different donor ionization energies. The model is shown graphically below.

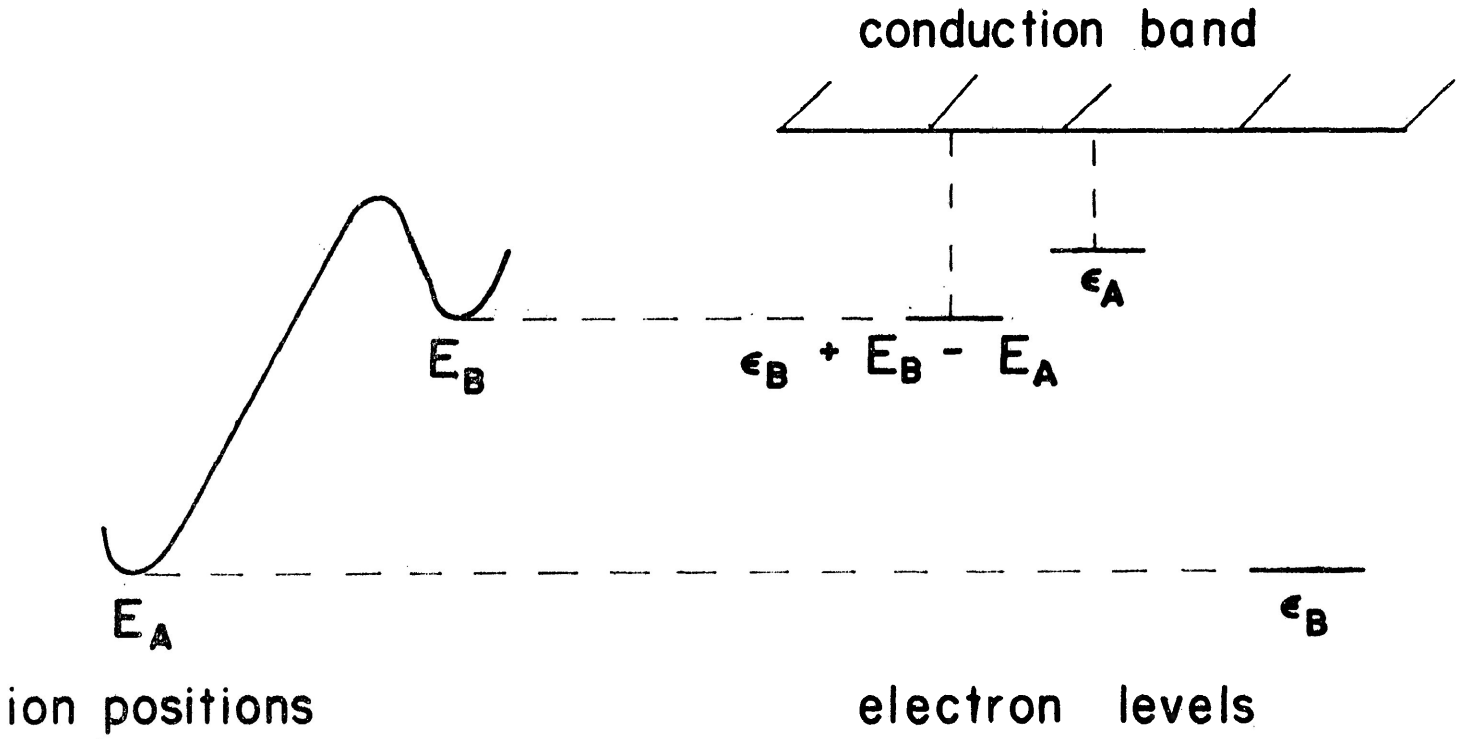

Figure 4

The barrier between sites A and B prevents ions moving between them at temperatures below $T_c \simeq 100^oK$. The donors can occupy positions A and B with corresponding ion energies E_A and E_B. The donor electron energies in these positions are ε_A and ε_B. We assume $E_A < E_B$ and $\varepsilon_A > \varepsilon_B$. The number of ions in positions A and B are N_A and N_B and $N_A + N_B = N_D$ = total impurity concentration. The number of electrons on donors in states A and B are n_A and n_B, and the number of available A and B sites per unit cell is G_A and G_B.

At thermal equilibrium the conditions for minimum free energy, valid above the transition, give

$$N_A = N\left[1 + \frac{G_B}{G_A}\exp\left(\frac{E_A-E_B}{kT}\right)\frac{1+2\exp\left(\frac{\varepsilon_F-\varepsilon_B}{kT}\right)}{1+2\exp\left(\frac{\varepsilon_F-\varepsilon_A}{kT}\right)}\right]^{-1} \qquad (1\text{-}5\text{-}2)$$

$$n_A = N_A\left[1 + \frac{1}{2}\exp\left(\frac{\varepsilon_A-\varepsilon_F}{kT}\right)\right]^{-1} \qquad (1\text{-}5\text{-}3)$$

ε_F is the Fermi energy level, and the electrons are assumed to have twofold spin degeneracy on donors.

We have also

$$n_A + n_B + n = n_o \qquad (1\text{-}5\text{-}4)$$

where n is the number of electrons in the conduction band, and n_o is the total number of donor electrons available.

The formulas giving N_A and n_A give N_B and n_B by simply reversing A and B in all expressions and subscripts.

The Fermi level can be calculated from

$$n = \frac{4}{3\sqrt{\pi}} N_c L_o^{3/2} \left[\frac{kT}{\epsilon_G} , \frac{\epsilon_F}{kT} \right] \tag{1-5-5}$$

$L_o^{3/2}$ is the generalized Fermi integral. ϵ_G is the band gap energy.

For the extrinsic range where $T > 100^oK$, Porowski calculates that the inequality

$$\epsilon_B << \epsilon_F << \epsilon_A \tag{1-5-6}$$

holds. The equations (1-5-2) and (1-5-3) may be simplified to give

$$N_B = n_B = N \left[1 + \frac{G_A}{2G_B} \exp \left(\frac{\epsilon_B + E_B - E_A - E_G}{kT} \right) \right] \tag{1-5-7}$$

$$n_A = 0 \tag{1-5-8}$$

where E_g is the energy gap at $\vec{k} = 0$.

Thus for $T > T_c$ we have ions moving from sites A to B with subsequent deionization in position B. If $G_A = G_B$

$$n_B = N\left[1 + \frac{1}{2}\exp\left(\frac{\varepsilon_B + E_B - E_A - E_G}{kT}\right)^{-1}\right] \qquad (1\text{-}5\text{-}9)$$

which is the usual expression for freeze-out onto a donor level with binding energy

$$\varphi = \varepsilon_B + E_B - E_A$$

and in the experimental results $E_2 = \varphi$.

When the temperature falls below the transition temperature the electrostatic barrier between ion positions prevents ion transfer from position A to B, thus N_A and N_B are fixed, level B will be fully populated with frozen-out electrons, and freeze-out onto level A begins. This will follow the normal pattern of freeze-out onto a level with binding energy ε_A and density N_A.

Porowski predicts relaxation time effects near the transition as a result of the electrostatic barrier slowing the rate at which ions can transfer from A to B.[14,15] He also points out that the freeze-out of level A below 100°K should be dependent on how the sample reached that point, i.e. whether the sample was cooled at the same pressure the readings are being taken at, or at some other pressure, which should affect N_A.

III. Carrier Freeze-out Anomaly: Alternative Model

An alternative explanation of the freeze-out anomaly may be obtained by considering compensation by acceptors in concentrations comparable to the donor concentration. It has been shown in the theory that a small concentration of acceptors in an n-type semiconductor will cause the freeze-out rate to double when the number of free electrons becomes less than the number of acceptors. This effect has not been observed in our measurements for any degree of freeze-out; the transition at $100^{o}K$ is in the reverse direction and the energy gap appears to decrease rather than increase as the temperature is lowered. However, it seems unlikely that the number of acceptor impurities is so small that it never exceeds the electron concentration, especially when this is reduced by several orders of magnitude. The possibility that a relatively large concentration of acceptor impurities is present was considered, and a mathematical analysis yields interesting results.

Eq. (1-2-16) gives a general solution for n under all doping conditions. This equation can be somewhat simplified by noticing that the term in

$$\frac{N_C N_V}{n} \exp(-\varepsilon_G)$$

in Eq. (1-2-15) corresponds to intrinsic carrier concentration and should be negligible in the temperature range of interest where the

semiconductor is extrinsic. A trial evaluation proved this to be the case. The equation then becomes

$$\frac{N_D N_G}{2n\ \exp(\varepsilon_D)+N_c} - n - \frac{nN_A}{2N_c\ \exp(\varepsilon_A-\varepsilon_G)+n} = 0 \qquad (1\text{-}5\text{-}10)$$

which can be expressed as

$$n^3 + \left[N_A + N_C\left(2\ \exp(\varepsilon_A-\varepsilon_G) + \frac{1}{2}\exp(-\varepsilon_D)\right)\right] n^2$$

$$+ \left[\frac{N_c}{2}(N_A-N_D)\ \exp(-\varepsilon_D) + N_c^2\ \exp(\varepsilon_A-\varepsilon_D-\varepsilon_G)\right]\ n$$

$$- N_c^2\ N_D\ \exp(\varepsilon_A-\varepsilon_D-\varepsilon_G) = 0 \qquad (1\text{-}5\text{-}11)$$

If the acceptor energy ε_A is small compared to the band gap ε_G then

$$\exp(\varepsilon_A-\varepsilon_G) \simeq \exp(-\varepsilon_G) \simeq 0$$

and the equation reduces to a quadratic

$$n^2 + n\left[N_A + \frac{N_c}{2}\exp(-\varepsilon_D)\right] + \frac{N_A-N_D}{2}\ N_c\ \exp(-\varepsilon_D) = 0 \qquad (1\text{-}5\text{-}12)$$

This can be shown to be identical to Eq. (1-2-12). It can be solved analytically, and the results are graphed for the following values:

$E_D = 0.1$ eV $\quad 1160/T = \varepsilon_D \quad N_D = 10^{20}/m^3$

$E_G = 0.32$ eV $\quad \varepsilon_G = 3717/T \quad N_c = 10^{19}T^{3/2}$

$N_A = N_D k/100$

k is the parameter specifying the degree of compensation.

It can be seen from Fig. 5 that for small values of k (light compensation) the kink predicted at $n = N_A$ occurs, and the curve becomes steeper at that point. For heavy compensation the freeze-out rate is almost constant over the entire range. The effect of increasing the acceptor concentration is merely to lower the absolute value of n. For k values greater than 100 the solution to the equation becomes negative. The physical reason for this is that when there are more acceptors than donors, the material becomes p-type.

The quadratic expression, however, only applies when one can assume all terms containing $\exp(-\varepsilon_G)$ are negligible. If the acceptor level is very high above the valence band the value $\varepsilon_G - \varepsilon_A$ may be comparable to the donor gap ε_D. We then use Eq. (1-5-10) which may be written as

Figure 5 Log n vs. 1/T calculated for various values of k ranging (from top to bottom)

k = 2

k = 50

k = 90

k = 99.5

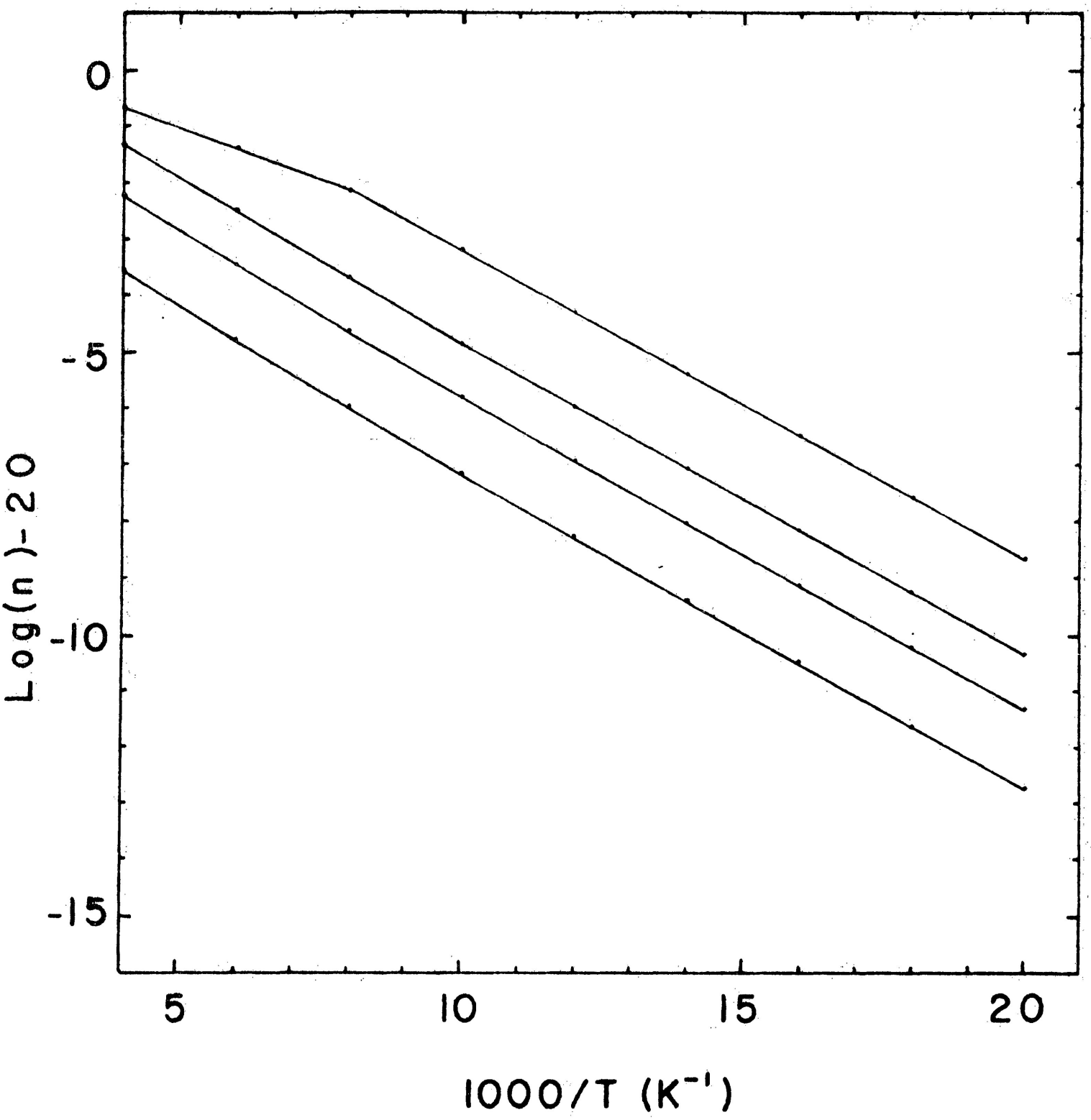
0
-5
-10
-15
Log(n)-20
5
10
15
20
1000/T (K⁻¹)

$$\frac{N_D}{n\frac{2}{N_c}\exp(\varepsilon_D)+1} - n - \frac{nN_D\frac{k}{100}}{2N_c\exp(\varepsilon_A-\varepsilon_G)+n} = 0$$

Defining

$$a = \frac{N_c}{2}\exp(-\varepsilon_D)$$

$$b = 2N_c\exp(\varepsilon_A-\varepsilon_G)$$

the equation becomes

$$n^3 + \left[N_D\frac{k}{100} + b + a\right]n^2 + \left[N_d\, a\left(\frac{k}{100} - 1\right) + ab\right]n$$

$$- N_d\, ab = 0 \qquad (1\text{-}5\text{-}13)$$

For $k < 100$ the coefficient of n is negative, and the equation has one sign change. For $k > 100$ the coefficient becomes positive, and the equation still has one sign change, but the form changes from ++-- to +++- suggesting some change in the character of the solution as k passes through 100. The fact that there is one sign change in either case indicates the presence of one positive root by Descarte's rule of signs.[35] It may also have two negative roots, but these have no physical significance.

Since Eq. (1-5-13) is a cubic it can actually be solved analytically. However, it proved technically simpler to program the solution as an iteration based on the Regula Falsi procedure.[36]

Solutions of n for a run to 1/T values were calculated for several energy gap values, and a range of k values near 100. The results of runs are plotted for the following energy gaps in Fig. 6:

$E_G - E_A = 238.6$ meV $\qquad E_D = 100$ meV

$E_G - E_A = 129$ meV $\qquad E_D = 43$ meV

At high temperatures above about 100^oK the slope of the curve corresponds to an effective energy gap of $\varphi_2 = (E_G - E_A) + E_D$ and below the transition we have $\varphi_2 = 2E_D$. The slope change occurs over a temperature range of about 10^oK, in agreement with our experimental plots of $n^2/(N_D-n)T^{3/2}$ (Figs. 9a, 9b, 10a and 10b) which are observed to deviate from linearity near 100^oK.

The kink in the theoretical curve is observed for a range of k values near k = 100. If k becomes too small the kink disappears, and if it approaches 100 too closely, the curve will become identical to the k = 100 curve which has a slope corresponding to the upper energy gap φ_2.

According to this theory then, the experimental results can be interpreted in the following manner:

Figure 6 Log n vs. 1/T calculated for two different sets of energy gap values

a E_A = 129 meV

E_D = 43 meV

b E_A = 238.6 meV

E_D = 100 meV

and various k values ranging (from top to bottom)

a k = 90

k = 100

b k = 90

k = 98.5

k = 99.5

k = 99.9

k = 100

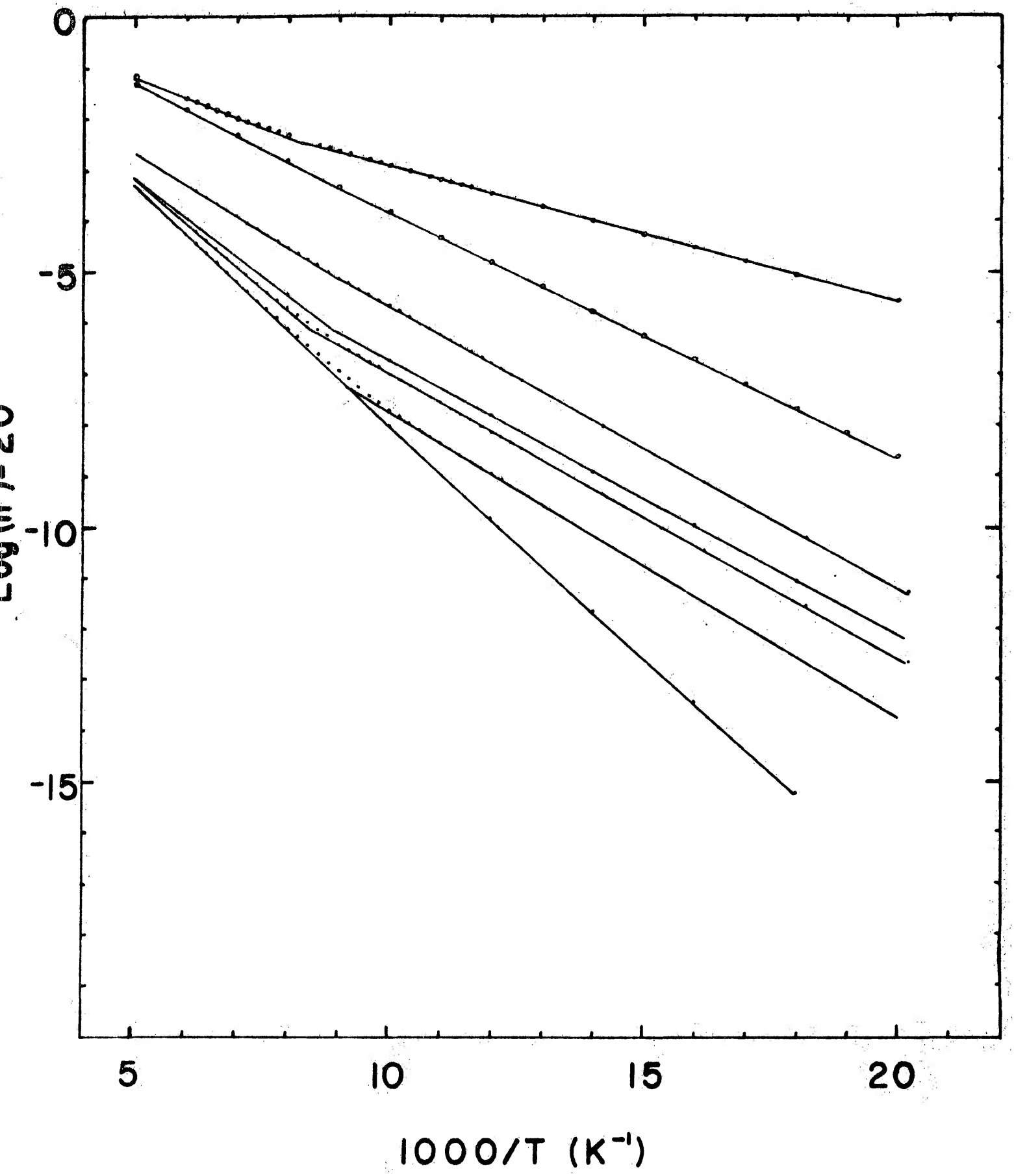
0
-5
-10
-15
5
10
15
20
1000/T (K⁻¹)

$$E_1 = 2E_D \quad Y_1 = 2\frac{dE_D}{dP} \tag{1-5-14}$$

$$E_2 = (E_G - E_A) + E_D \quad Y_2 = \frac{dE_D}{dP} + \frac{dE_A}{dP} \tag{1-5-15}$$

where E_1 and E_2 are the experimentally observed lower and upper temperature energy gaps, and Y_1 and Y_2 are their pressure derivatives. All pressure derivatives are relative to the conduction band.

Chapter 2

Sample Preparation and Experimental Techniques

Detailed descriptions of the pressure vessel and sample preparation are to be found in the thesis of S.M. Fong.[26] A brief account of sample preparation and mounting will be given here along with any new techniques, and the experimental methods discussed.

2-1. Sample Preparation

The specimens of n and p-type InSb used were cut from single crystal ingots. They measured approximately 0.5x1.5x1.5 mm. After cleaning and etching, electrical connections were made to the sample with 0.003 inch platinum wire. Copper wires were soldered to the platinum, direct connections by copper wires would result in copper contamination of the sample since copper has a high diffusion coefficient in InSb and most other semiconductors.

The platinum wires were soldered onto the samples in earlier work using indium solder containing 2% tellurium. The tellurium reduces the possibility of forming a p-n junction at the contact. Soldering with this technique proved fairly difficult and the contacts were not strong, so an alternative method was tried, namely capacitive discharge welding. In this method the sample is connected electrically to a capacitor, and the platinum wire to the other side

of the capacitor, which is charged to an appropriate voltage. The wire is then brought in contact with the sample where contact is to be made. The energy of the discharge is deposited mostly in the contact area, resulting in melting and fusing of the wire and InSb. The contact so produced is generally stronger than that achieved with solder, although it must be tested to make sure it is not subject to fatigue when the wire is bent.

The capacitor used by us with most success was a 750 μf 120 volt electrolytic, which was charged through a current limiting resistor from a 0-70 volt variable D.C. supply. The voltage range for successful welds lay between about 10 and 40 volts. Initial attempts should be made at low voltage to avoid sample damage by extensive melting.

In our work the sample was held in stainless steel tweezers which were connected to the capacitor. The platinum wire was held in a metal bit on a movable platform, and the contacting was viewed through a microscope. The method was successfully used on a variety of semiconductor samples; the only problems arose in materials with very high resistivities which limited the discharge of the capacitor.

After the leads were attached the sample was tested electrically to ensure that there were no p-n junction effects at the contacts, and that the contact symmetry was high enough to give an f factor less than 2. Both soldered and welded contacts were equally satisfactory in their electrical characteristics.

2-2. Experimental Methods

Hall and resistivity measurements were made on samples of n and p-type InSb using the Van der Pauw technique described in section 1-4. The measuring current was passed through a 1Ω standard resistor in series with the sample, and the voltage generated across this resistor provided a measure of the current. A Hewlett-Packard Model 419A Null DC voltmeter was used to measure both the sample voltage and the voltage across the standard resistor.

In addition to changing the lead configurations as required by the Van der Pauw technique, the measuring current was reversed and two sets of readings taken for Hall and resistivity measurements in order to eliminate thermoelectric contact potentials. The magnetic field was also reversed in Hall measurements and the paired sets of data averaged. This ensured that no other thermomagnetic effect contributed to the Hall reading, except possibly the Ettingshausen effect. This has the same current and field dependence as the Hall effect, but it is small compared to the Hall effect and requires a thermal gradient, which should have been eliminated by controlling the temperature at each setting for 10 to 30 minutes before taking a reading.

In some of our high electric field studies (high carrier density-high current) we encountered transient effects which we

ascribe to sample heating. In order to minimize this problem, pulse measurements were used when necessary. A Hewlett-Packard 8011A pulse generator was used as the current source, and an oscilloscope was used to measure the pulse voltage across the standard resistor and across the sample. This method eliminated the need to reverse the measuring current thus halving the number of readings to be taken. The method was successful provided the pulse length was long enough for all LCR effects to die out since the sample did not represent a well matched load, particularly in the freeze-out regime where sample resistivity was very high. The pulse length was typically 1 millisecond and the duty cycle 1 part in 100.

One of the problems in pressure measurements carried out over a large temperature range is differential contraction pressure loss. The contraction rate of the metal is usually less than that of the pressure fluid, leading to a reduction of pressure during cool down. To obtain an estimate of this pressure loss we made a series of constant temperature variable pressure measurements of the sample resistivity at $297^{o}K$, $198^{o}K$ (dry ice in acetone) and $77^{o}K$. At room temperature the sample was pressurized in stages with readings taken at each step, and then de-pressurized in a similar manner. When a plot of ρ versus applied pressure was made, a hysteresis loop was observed in that the pressure on the sample appeared higher during de-pressurization. This was taken to be due

to internal friction in the pressure vessel. The width of the hysteresis curve was about 1.5 kbar and the true pressure was assumed to lie in the middle. At lower temperatures the pressure fluid was frozen and it was possible only to increase the pressure but not to decrease it, so the width of the hysteresis loop had to be assumed.

During subsequent constant pressure variable temperature runs the resistivity values were measured at these temperatures (297^{o}, 198^{o}, 77^{o}K) and the pressure determined from the graphs of resistivity vs. pressure. The pressure was found to have fallen about 15% at 198^{o}K and 25% at 77^{o}K. Below 77^{o}K thermal expansions are small so the pressure was assumed to be constant.

Chapter 3

Results and Discussions

3-1. Temperature Dependent Carrier Number in n-InSb

The Hall voltage as a function of temperature has been measured from 297°K to about 10°K for two samples of n-type InSb at pressures in the range of 0 to 15 kbar. The samples are referred to as sample #1 and sample #2 and the donor concentrations taken as the number of free electrons measured at low pressure and 77°K are

$$N_{D1} = 9.09 \times 10^{19}/m^3$$

$$N_{D2} = 8.0 \times 10^{19}/m^3$$

Figs. 7 and 8 show the temperature dependence of R_H for Samples 1 and 2. Freeze-out of electrons onto impurities is observed for pressures exceeding 8 kbar. The transition described by Porowski is clearly visible in this range, manifesting itself as a rapid slope change in a plot of R_H vs. temperature in the vicinity of 100°K. Below the transition the freeze-out rate is decreased as if the donor activation energy is smaller, and the number of donors also appears to decrease.

Figure 7 A semilog plot of n vs. T for n-InSb sample #1 at various pressures.

● P = 8 kbar

○ P = 11.6 kbar

■ P = 12.2 kbar

▲ P = 13.4 kbar

X P = 14.7 kbar

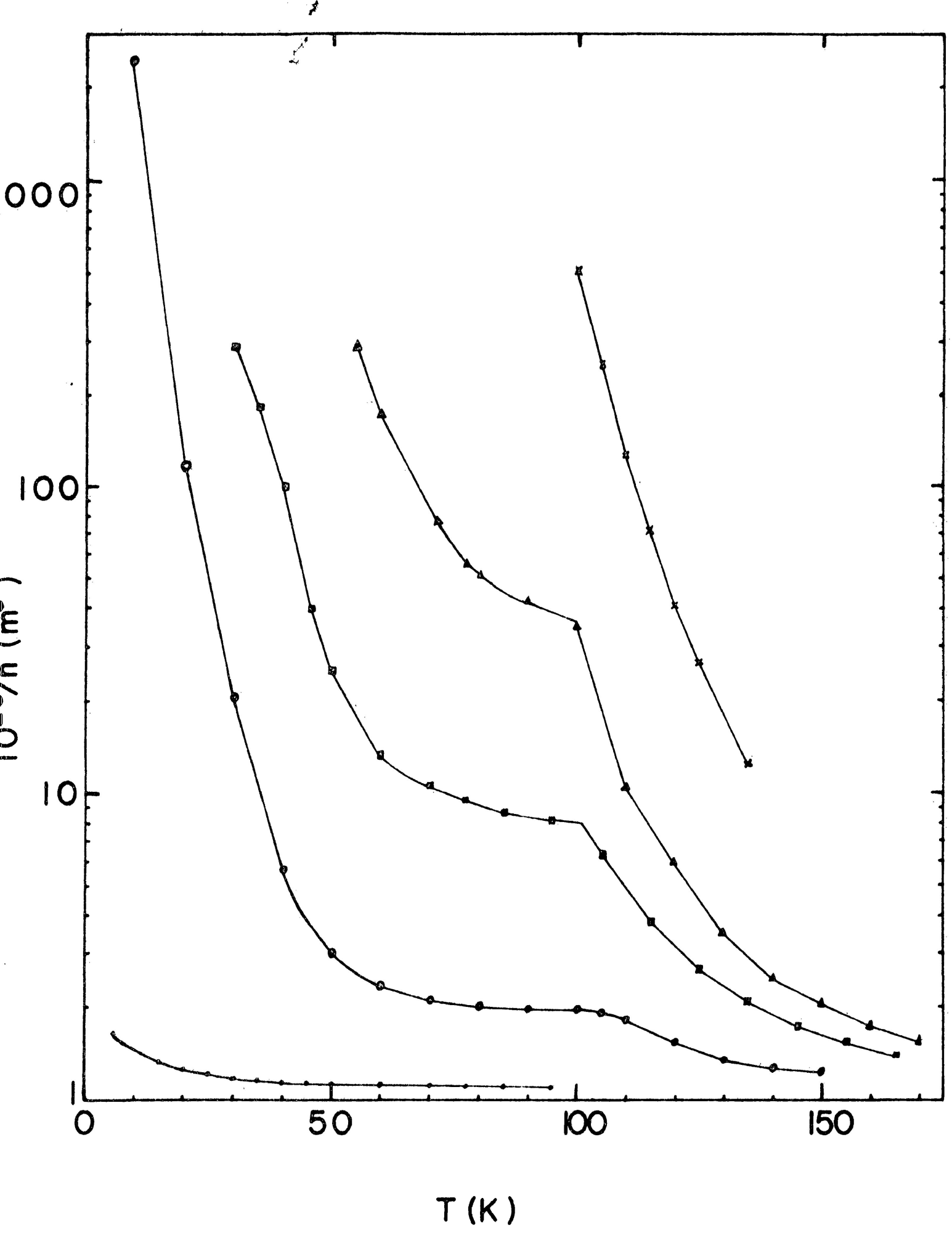
000
100
10
1
0
50
100
150
T (K)

Figure 8 A semilog plot of n vs. T for n-InSb sample #2 at various pressures.

● P = 0 kbar

○ P = 8.0 kbar

■ P = 10.9 kbar

▲ P = 11.3 kbar

□ P = 12.5 kbar

X P = 15.0 kbar

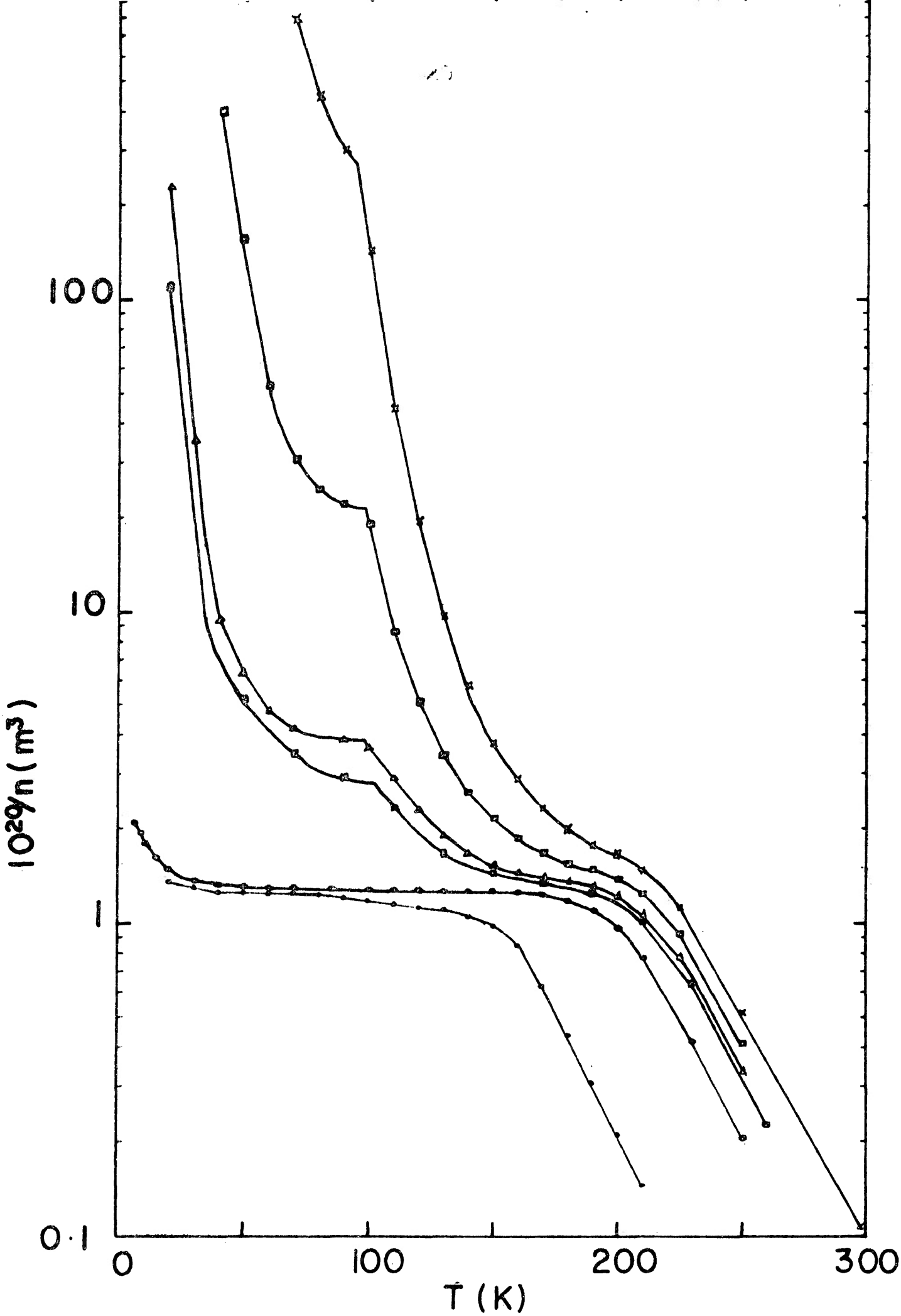
100
10
1
0·1
$10^{29}/n\,(m^3)$
0
100
200
300
T (K)

At pressures below 8 kbar the carrier number in the extrinsic range stays almost constant down to temperatures of the order of 10^{0}K and then decreases in a manner suggesting freeze-out of the electrons onto a donor level with very low activation energy.

3-2. Analysis of Donor Energy Gaps

The data shown in Figs. 7 and 8 was used to determine the pressure dependent donor gaps for the two samples, for both the upper and lower temperature ranges. Eq. (1-2-10) gives

$$\frac{n^2}{(N_D-n)N_c} = B \exp\left(\frac{-E_D}{k_B T}\right) .$$

Since B is a constant and $N_c \propto T^{3/2}$ we have

$$\frac{n^2}{(N_D-n)T^{3/2}} \propto \exp\left(\frac{-E_D}{k_B T}\right)$$

or

$$\log\left[\frac{n^2}{(N_D-n)T^{3/2}}\right] \propto \frac{-E_D}{k_B T} \log(\exp) \qquad (3\text{-}2\text{-}1)$$

Thus a semilogarithmic graph of $n^2/(N_D-n)T^{3/2}$ against 1/T should give a straight line, and the energy gap E_D is determined from

$$\frac{d \log\left[\frac{n^2}{(N_D-n)T^{3/2}}\right]}{d(1/T)} = -\frac{E_D}{k_B} \log(\exp) \qquad (3\text{-}2\text{-}2)$$

The value of N_D used in analyzing the donor gap above 100^oK (which we will call E_2) is the same as that quoted for the sample impurity concentration in section 3-1. Below 100^oK, however, the donor gap (E_1) must be determined using a new value of N_D which is the value of carrier number at which the freeze-out curve below the transition appears to be levelling off at as the temperature is raised. As can be seen in Figs. 7 and 8 this value is most readily determined in the lower pressure freeze-out curves where the carrier number below 100^oK is practically constant with temperature for some distance. At higher pressures the value of N_D is less apparent and trial and error may have to be used to produce a straight line. However, when freeze-out becomes advanced and $n << N_D$ the term $(N_D - n)$ is practically constant and the accuracy of the N_D value chosen will not affect the linearity of the points, or the value of E_1 that is calculated using them.

Plots of $\log(n^2/(N_D-n)T^{3/2})$ versus $1/T$ for samples 1 and 2 are shown in Figs. 9a, 9b, 10a and 10b. As can be seen from Figs. 9a and 10a the high temperature data falls into a straight line between about 150^oK and 100^oK. Deviations from linearity at high temperature are caused by the onset of intrinsic conduction, and at the lower

temperature end by the onset of the transition. Figs. 9b and 10b show the results of the low temperature donor gap analysis. Again the observations deviate from linearity near the transition. Deviations at the low temperature ends are probably due to practical difficulties in making accurate measurements when the Hall resistivity becomes very large.

The energy gaps E_1 and E_2 were determined from these graphs, using Eq. (3-2-2). The values of these energies are plotted against pressure in Fig. 11 to find the pressure derivatives of E_1 and E_2 . Assuming that the donor levels continue rising after they enter the conduction band, we were able to predict the values E_{01} and E_{01} which are the values of E_1 and E_2 at zero pressure relative to the conduction band minimum. The results obtained for E_{01} and E_{02} , and their pressure derivatives Y_1 and Y_2 are:

E_{01} = 125 meV $\quad$ Y_1 = -13.3 meV/kbar

E_{02} = 218.5 meV $\quad$ Y_2 = 26.0 meV/kbar

These agree quite well with values quoted by Porowski:[13]

E_{01} = 85 meV $\quad$ Y_1 = -10.5 meV/kbar

E_{02} = 145 meV $\quad$ Y_2 = -20.0 meV/kbar

Figure 9a A semilog plot of $n^2/(N_D - n)T^{3/2}$ vs. $10^3/T$ for n-InSb sample #1 at temperatures above 100^oK and various pressures.

- ● P = 11.6 kbar
- ○ P = 12.2 kbar
- ■ P = 13.4 kbar
- X P = 14.7 kbar

Dashed lines extend the parts of the curves for energy gap determination.

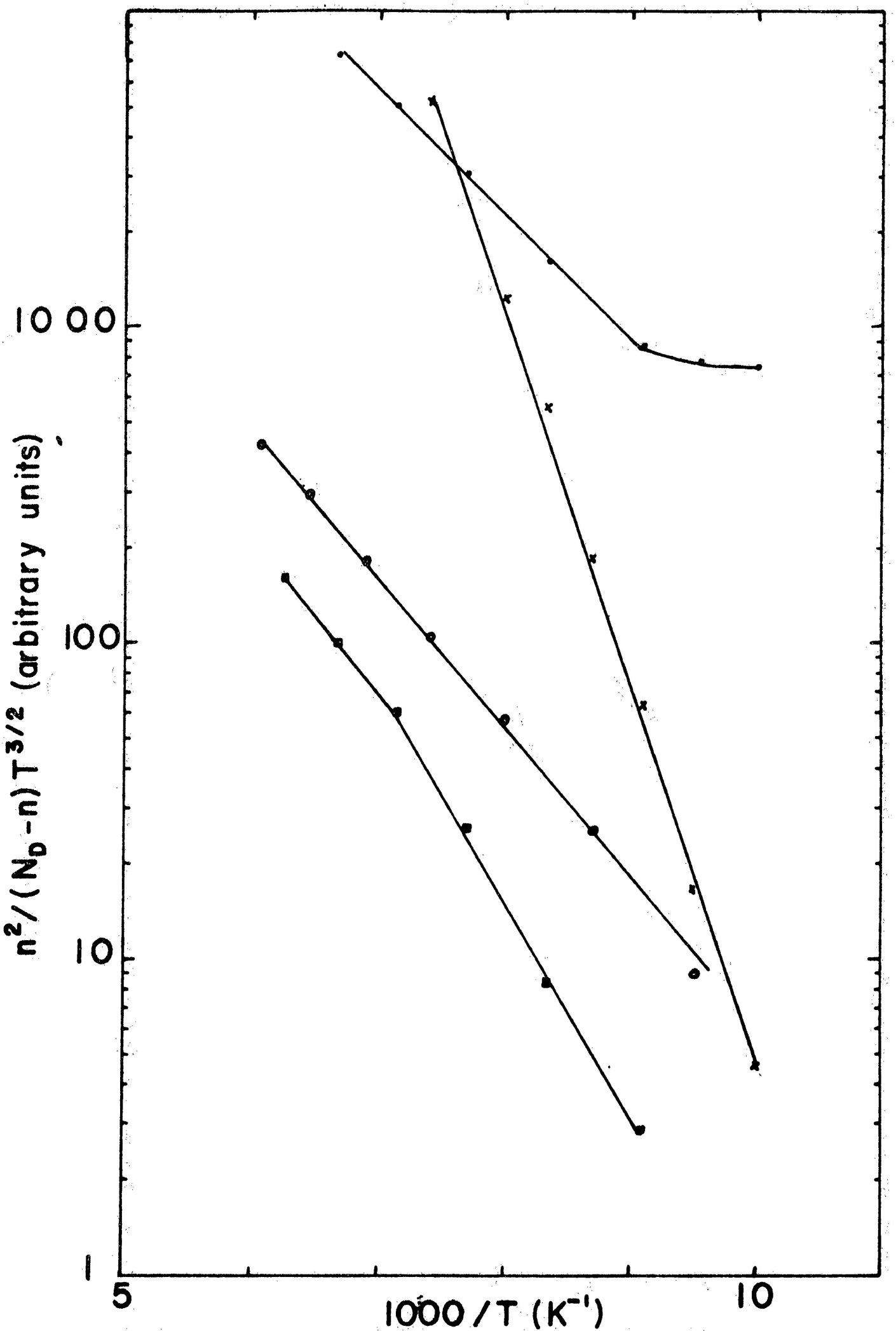
1000
100
10
1
$n^2/(N_D-n)T^{3/2}$ (arbitrary units)
5
10
1000/T (K^{-1})

Figure 9b A semilog plot of $n^2/(N_D - n)T^{3/2}$ vs. $10^3/T$ for n-InSb sample #1 at temperatures below 100^oK and various pressures.

- ● P = 11.6 kbar
- ○ P = 12.2 kbar
- ■ P = 13.4 kbar

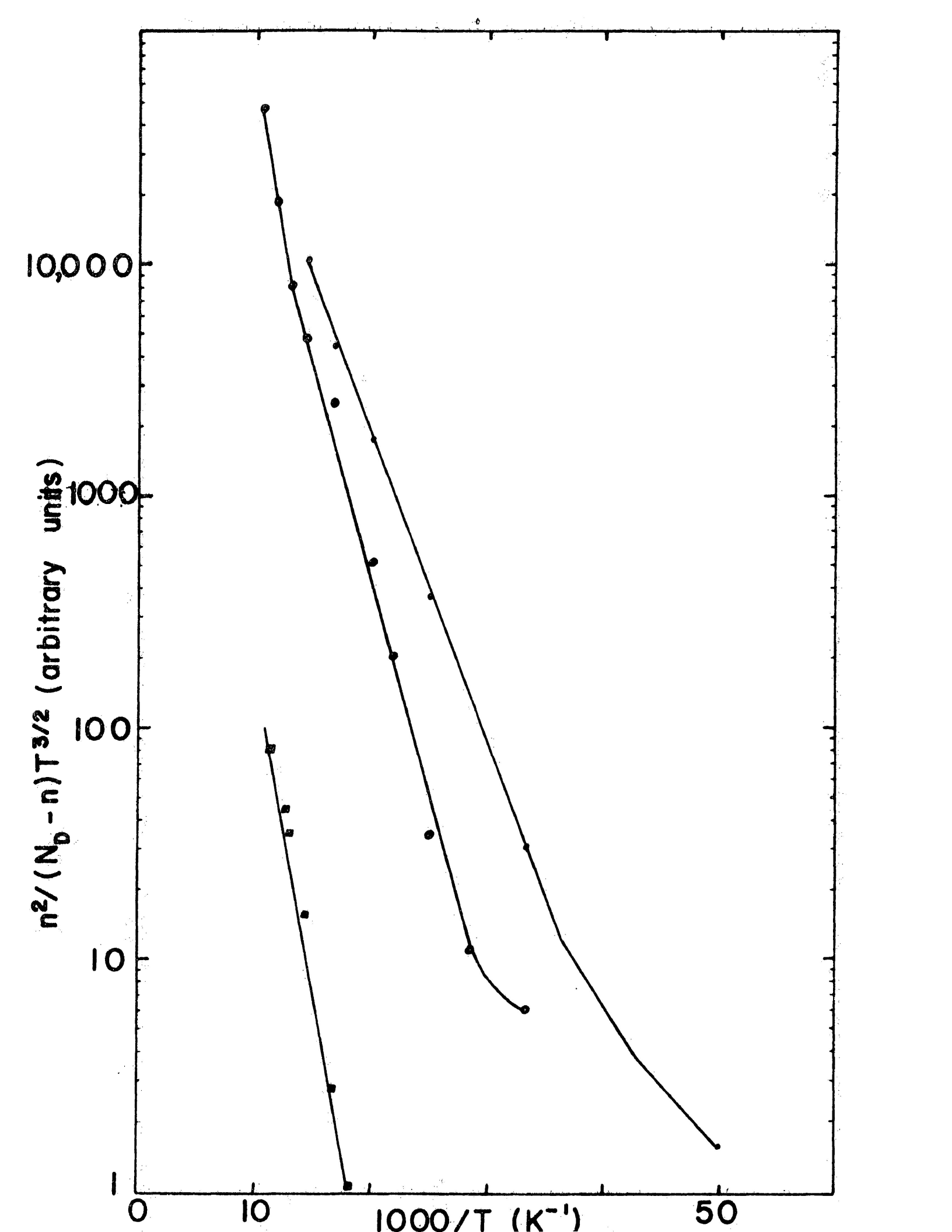
10,000
1000
100
10
1
$n^2/(N_D - n)T^{3/2}$ (arbitrary units)
0
10
1000/T (K^{-1})
50

Figure 10a A semilog plot of $n^2/(N_D - n)T^{3/2}$ vs. $10^3/T$ for n-InSb sample #2 at temperatures above 100^oK and various pressures.

- ● P = 10.9 kbar
- ○ P = 11.3 kbar
- ▲ P = 12.5 kbar
- X P = 15.0 kbar

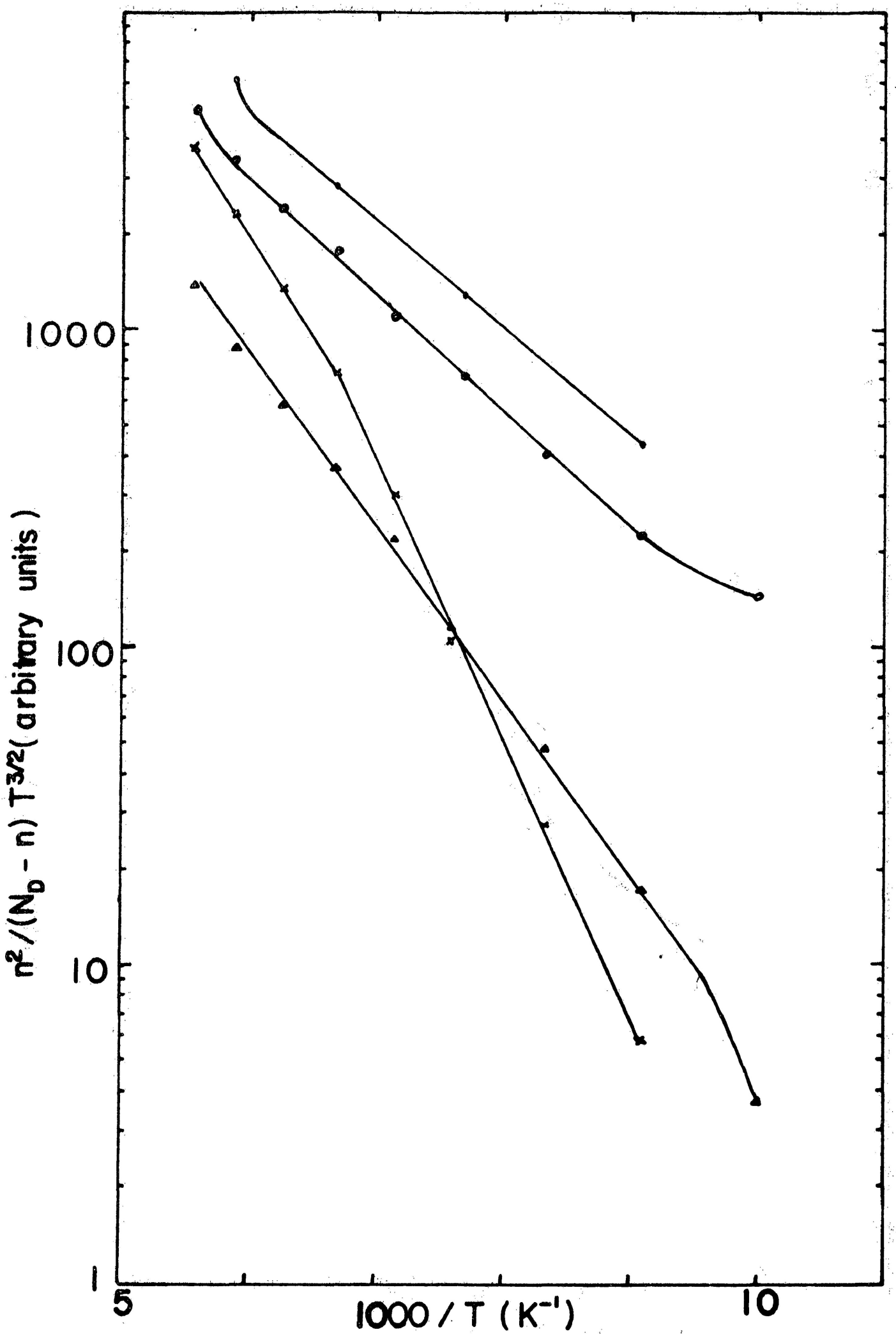
1000
100
10
1
5
10
1000 / T (K⁻¹)
n²/(N_D - n) T^3/2 (arbitary units)

Figure 10b A semilog plot of $n^2/(N_D - n)T^{3/2}$ vs. $10^3/T$ for n-InSb sample #2 at temperatures below 100^oK and various pressures.

- ● P = 10.6 kbar
- ○ P = 11.3 kbar
- ■ P = 12.5 kbar
- X P = 15.0 kbar

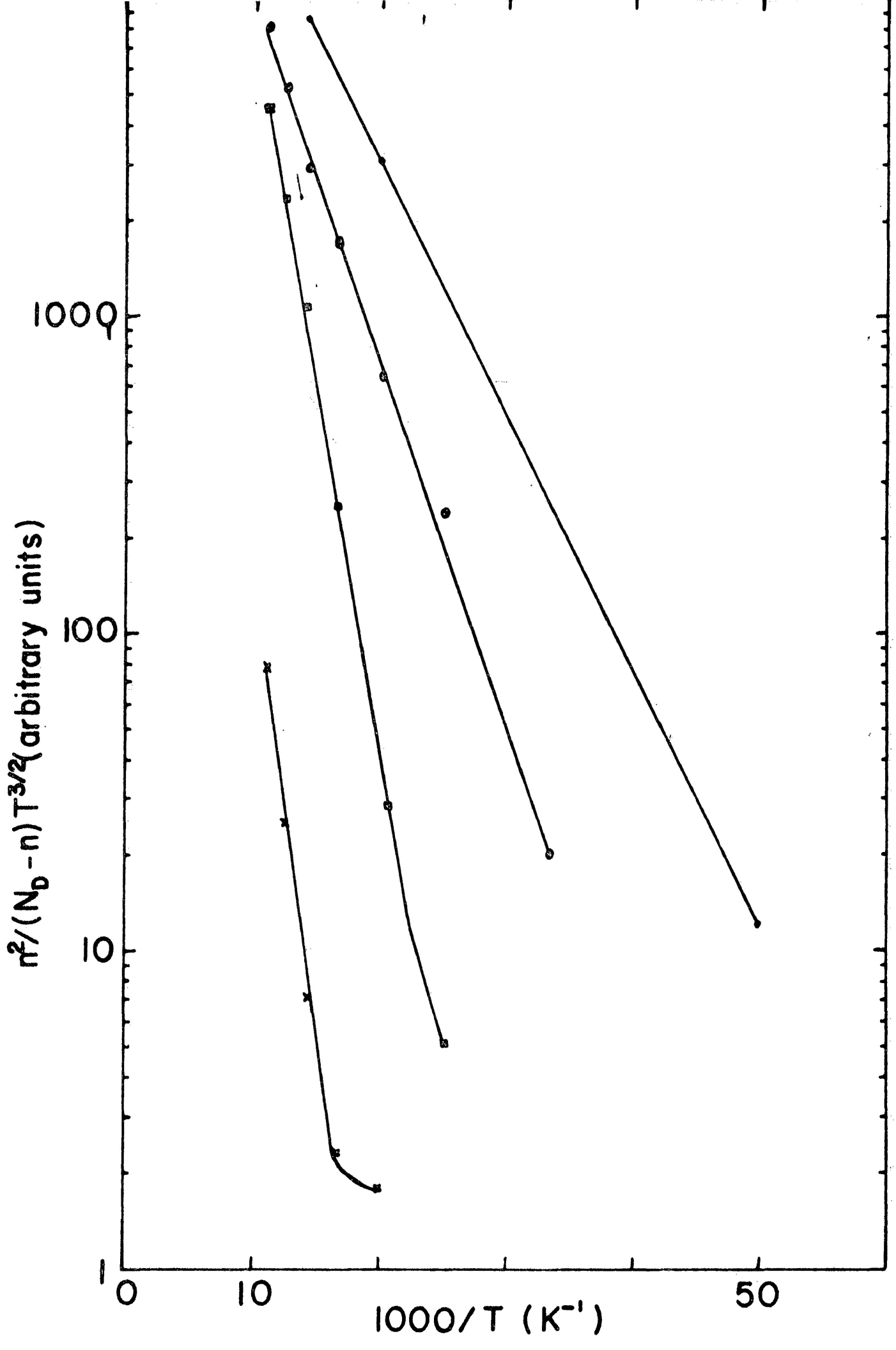
1000
100
10
1
0
10
50
1000/T (K⁻¹)
n²/(N_D - n) T^{3/2} (arbitrary units)

Figure 11 A plot of E_D vs. pressure P for the two energy gaps E_1 and E_2. Points marked ▲ are from sample #1 and points marked ● are from sample #2.

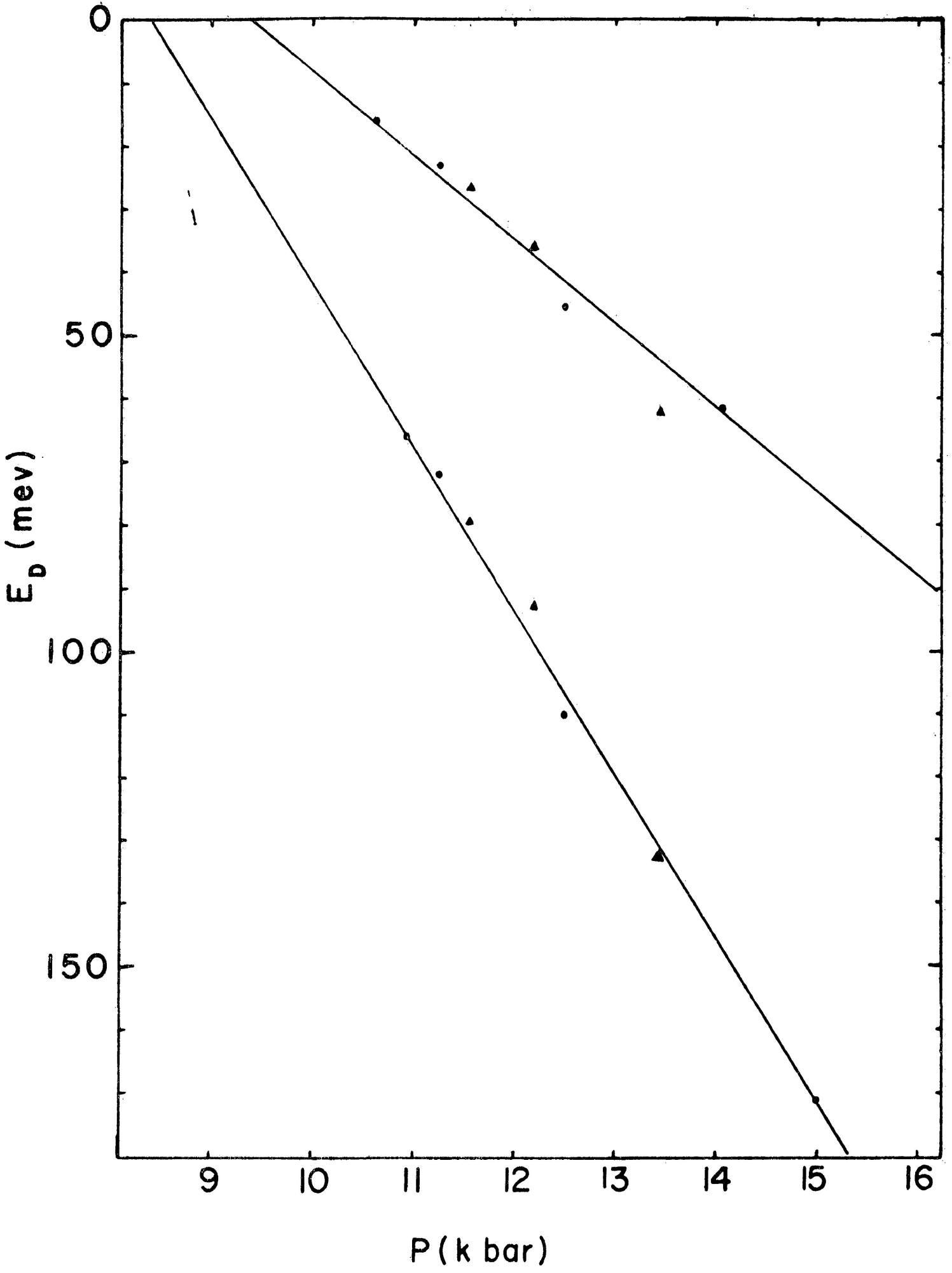
0
50
100
150
E_D (mev)
9
10
11
12
13
14
15
16
P (k bar)

According to the theory of Porowski the lower donor gap E_1 is caused by freeze-out onto a donor level with this activation energy, while E_2 is caused by freeze-out onto a lower donor level where the activation energy is determined by both electronic and atomic processes, thus the pressure derivative of this level cannot be related to any purely electronic effect such as the pressure derivatives of band gaps. The pressure derivative of the E_1 level can be so related since it is determined by electronic processes. Porowski associates this level with the L minimum which has a pressure derivative of 8.3 meV/kbar relative to the valence band. However, as we are dealing with donor states we are interested in the pressure derivative with respect to the conduction band minimum, which is -5.7 meV/kbar for the L minimum.

Interpreting the results on the basis of our theory gives us values for the hypothetical donor and acceptor levels, and their pressure derivatives. Using Eqs. (1-5-15) and (1-5-16) and our experimental data we find

$$E_D = 62.5 \text{ meV} \qquad Y_D = -6.65 \text{ meV/kbar}$$
$$E_A = 156 \text{ meV} \qquad Y_A = -19.35 \text{ meV/kbar}$$

Using Porowski's values for the activation energies and their pressure derivatives, the results are

E_D = 42.5 meV Y_D = -5.25 meV/kbar

E_A = 102.5 meV Y_A = -14.75 meV/kbar

It can be seen that the pressure derivatives of the donor level for both sets of results lie very close to the pressure derivative of the L band relative to the conduction band (-5.7 meV/kbar).

The pressure derivative of the acceptor level using Porowski's data is close to the pressure derivative of the valence band relative to the conduction band (-14 meV/kbar) while our data puts the value somewhat higher.

Thus the assumed donor and acceptor levels in our theory have pressure derivatives suggesting that they are connected with the L band minimum and valence band maximum respectively.

In the next section we show that the acceptor level in p-type InSb is nearly fixed with respect to the valence band under pressure, although as a different type of acceptor is involved this cannot be taken as proving that E_A is connected with the valence band.

3-3. Temperature Dependent Carrier Number and Acceptor Gap in p-type InSb

Hall measurements were made on a p-type sample of InSb at pressures between zero and 8 kbar. The results are shown in Fig. 12. The change from extrinsic to intrinsic conduction occurs when $n\mu_n^2 = p\mu_p^2$ and as the ratio of $\mu_n^2/\mu_p^2 \simeq 6400$ the hole concentration must be

Figure 12 A semilog plot of R_H/e vs. T for p-InSb at various pressures.

● P = 1.6 kbar

X P = 3.1 kbar

○ P = 4.4 kbar

■ P = 7.8 kbar

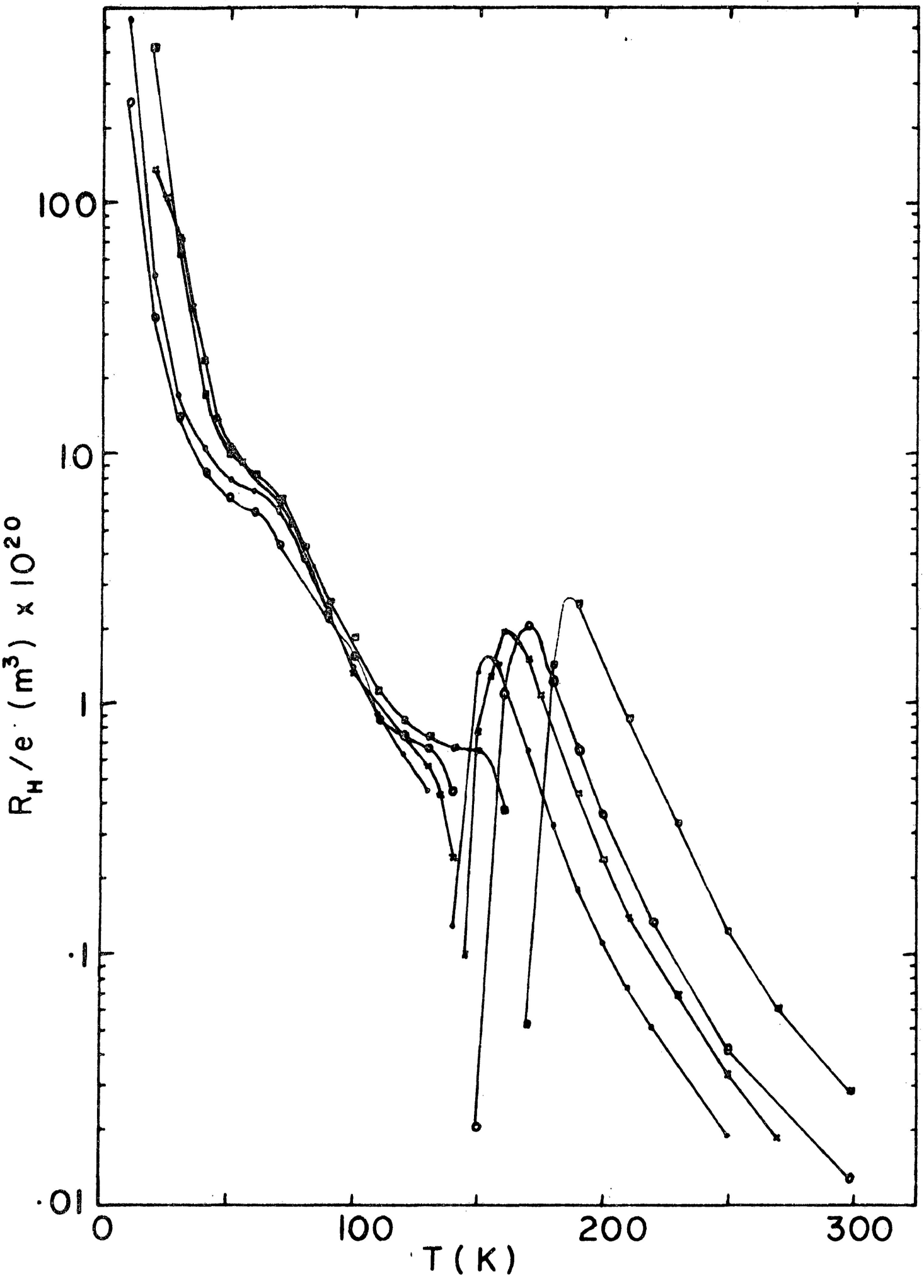
100
10
1
·1
·01
$R_H/e\cdot(m^3)\times10^{20}$
0
100
200
300
T(K)

at the extrinsic limit when the transition occurs, i.e., $p = N_A$. The temperature at which the material changes from n to p-type moves up with pressure because of the increasing band gap.

Determination of extrinsic carrier number is difficult because freeze-out of the acceptor level has apparently begun when the material becomes extrinsic. As mentioned in the theory (section 1-4) it is safe to assume extrinsic behavior for temperatures twenty degrees below the transition from n to p-type. The donor freeze-out equation (1-2-10) can be applied to acceptor freeze-out:

$$\frac{p^2}{(N_A-p)N_V} = B \exp\left[\frac{-E_A}{k_B T}\right]$$

where $N_V = 2(2\pi m_p^* k_B T/h^2)^{3/2}$ m_p^* is the effective mass of the holes.

An expression for E_A can be derived in the same way as for E_D (section 3-2).

$$\frac{d \log\left[\frac{p^2}{(N_A-p)T^{3/2}}\right]}{d(1/T)} = - \frac{E_A}{k_B} \log(e) \qquad (3\text{-}3\text{-}1)$$

For advanced freeze-out $N_A >> p$ and the derivative of $(N_A - p)$ may be ignored leaving

$$\frac{d \log(p^2 T^{-3/2})}{d(1/T)} = - \frac{E_A}{k_B} \log(\exp)$$

or

$$\frac{d \log(pT^{-3/4})}{d(1/T)} = - \frac{E_A}{k_B} \frac{\log(\exp)}{2} \qquad (3\text{-}3\text{-}2)$$

There is, however, another complication in that there are two types of holes contributing to the conduction processes. From the theory, Eq. (1-4-9) gives

$$R_H = \frac{1}{p_2} \left[\frac{Y_H}{e} \frac{b^2 x + 1}{(bx + 1)^2} \right] \qquad (1\text{-}4\text{-}9)$$

$$b = \mu_1/\mu_2 \quad x = p_1/p_2$$

The ratio of the concentrations of the two types of holes is

$$x = p_1/p_2 = N_{V1}/N_{V2} = \left(\frac{m_1^*}{m_2^*} \right)^{3/2}$$

The mobility ratio is also determined by the effective masses of the two types of holes, since effective mass comes into the mobility formulas. In the temperature range of 150°K to 70°K polar optical scattering is probably the dominant scattering mechanism. For this process[28]

$$\mu_{op} \propto \left(\frac{m_o}{m^*}\right)^{3/2} \quad \therefore \quad \mu_{op} \propto m^{*-3/2}$$

$$\therefore \quad b = \mu_1/\mu_2 \left(\frac{m_1^*}{m_2^*}\right)^{3/2}$$

Using these relations the equation (1-4-9) simplifies to

$$R_H = \frac{1}{p_2}\left(\frac{Y_H}{e}\,\frac{\left(\frac{m_1^*}{m_2^*}\right)^{3/2} + 1}{4}\right) \tag{3-3-3}$$

From the band structure formulas in section 1-1 we find that the curvature of the light hole band, and hence the effective mass, is proportional to the band gap energy just as it is for the conduction band. The heavy hole band is independent of the band gap and the effective mass is equal to 0.6 m_o .

If we let p_1 represent heavy holes and p_2 the light holes, then as pressure increases the value of $(m_1^*/m_2^*)^{-3/2}$ increases from a zero pressure value of about $\frac{1}{125}$ to about $\frac{1}{60.5}$ at 8 kbar. Since both of these numbers are much smaller than 1 it seems they can be ignored in Eq. (3-3-3). Thus

$$R_H \simeq 1/p_2 \frac{Y_H}{4e} = \frac{x}{p_1} \frac{Y_H}{42} = \left(\frac{m_1^*}{m_2^*}\right)^{3/2} \frac{Y_H}{4p_1 e} \qquad (3\text{-}3\text{-}4)$$

The heavy hole band represented by p_1 is largely responsible for freeze-out effects since it has a much larger density of states, while the light holes play the dominant role in the Hall effect due to their higher mobility. For the purposes of energy gap determination we are interested in the temperature derivative of R_H and p_1. We know that m_1^* stays constant, while m_2^* will vary slightly since it is proportional to the band gap energy, and this has a small temperature derivative (0.29 meV/^oK), but as this would cause only about a 10% change in E_G and m_2^* over a 100^oK range compared to freeze-out over several orders of magnitude, it seems safe to ignore temperature variation in the effective mass of holes as we did in the case of electrons.

To analyze our data we plotted $(R_H T^{3/4})^{-1}$ against 1/T and used the slope to calculate the energy of the acceptor level using Eq. (3-3-2). The graphs are shown in Figs. 13a and 13b. The resulting values of E_A are graphed against pressure in Fig. 14. The points being somewhat scattered, we used a least squares fit and found for the zero pressure acceptor gap and its pressure derivative.

Figure 13a A semilog plot of $(R_H T^{3/4})^{-1}$ vs. $10^3/T$ for p-InSb at pressures ranging (from top to bottom)

P = 4.4 kbar

P = 3.1 kbar

P = 1.6 kbar

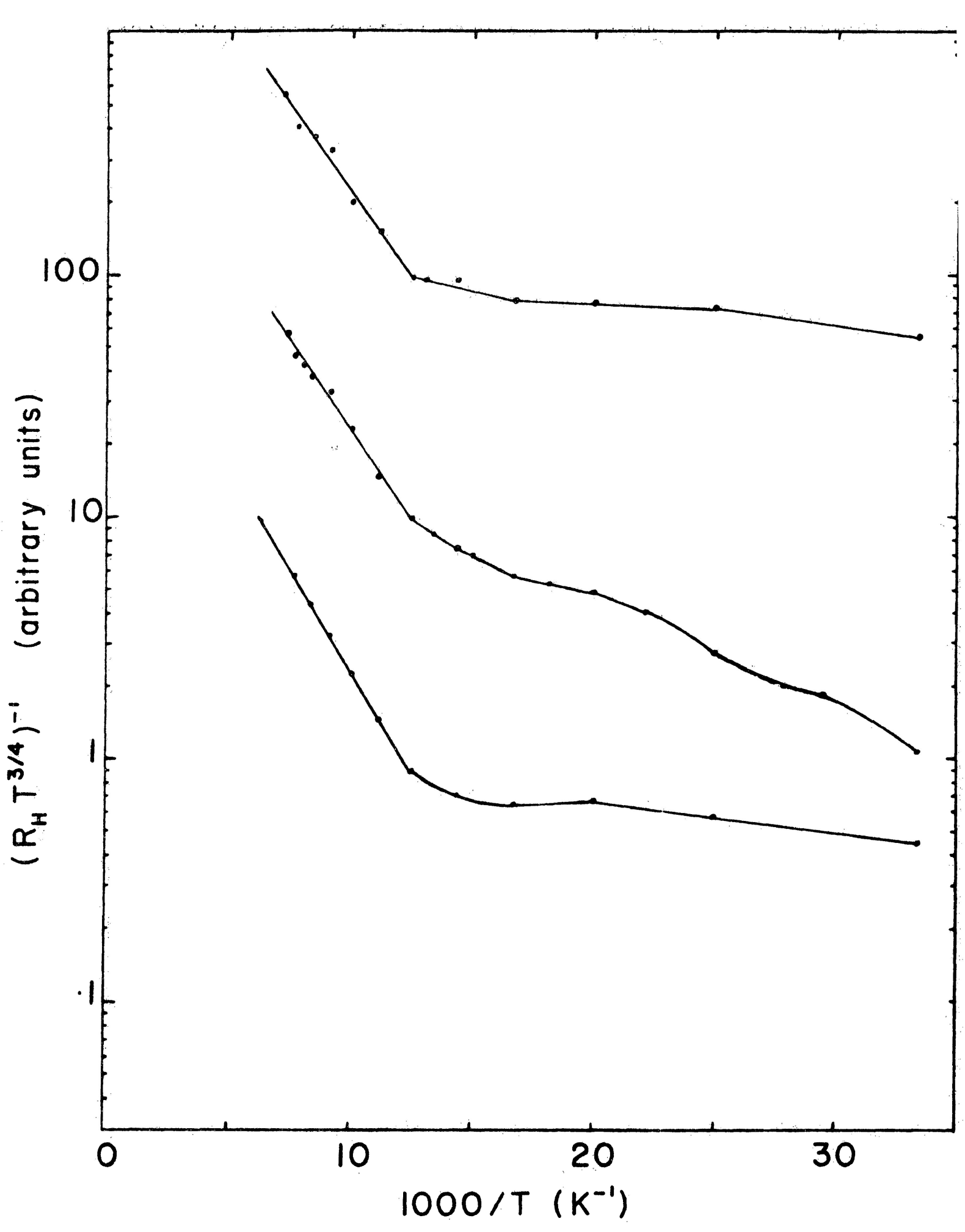
100
10
0
10
20
30
$(R_H T^{3/4})^{-1}$ (arbitrary units)
1000/T (K^{-1})

Figure 13b A semilog plot of $(R_H T^{3/4})^{-1}$ vs. $10^3/T$ for p-InSb at pressures ranging (from top to bottom)

P = 7.8 kbar

P = 6.3 kbar

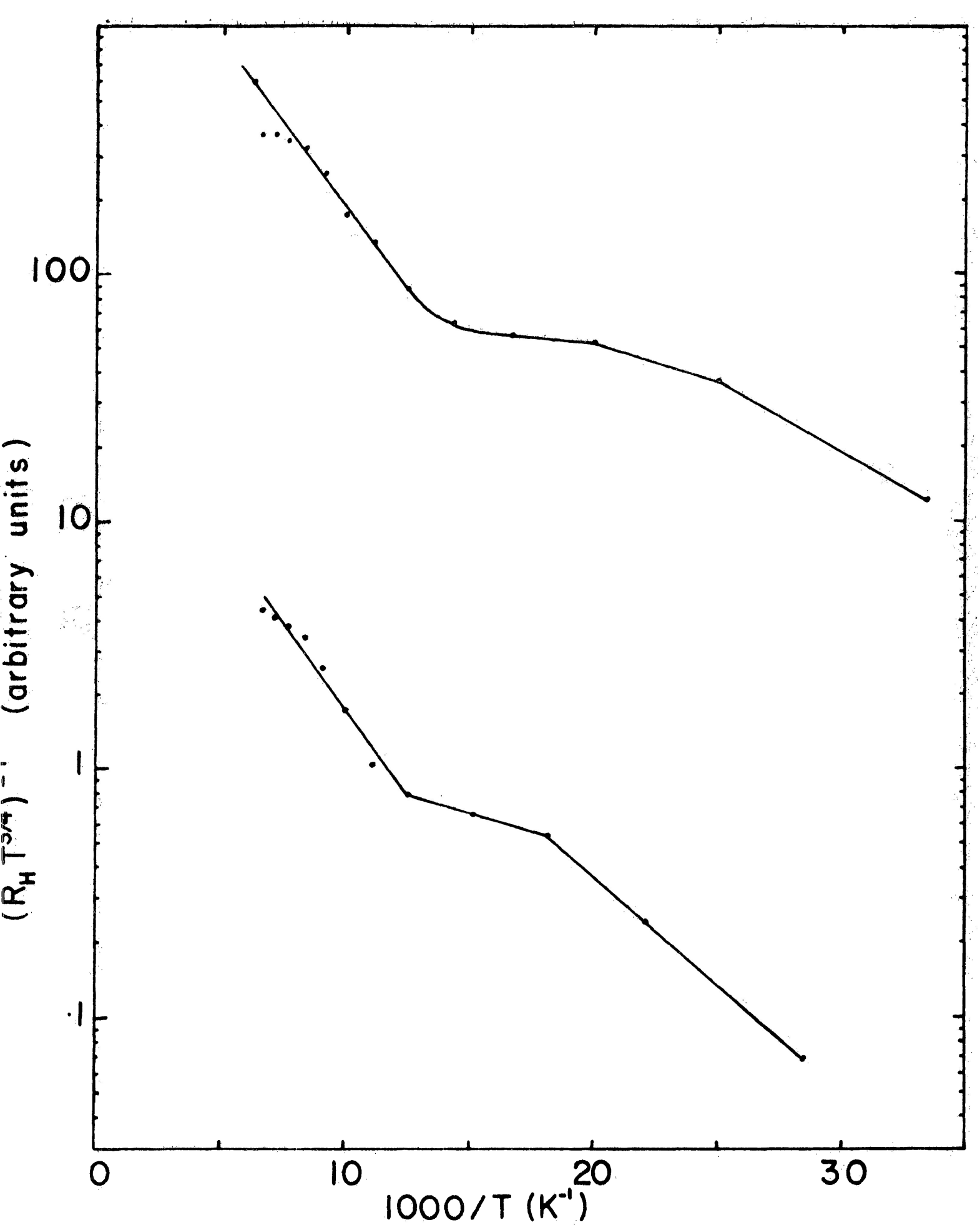
100
10
1
·1
$(R_H T^{3/4})^{-1}$ (arbitrary units)
0
10
20
30
1000/T (K^{-1})

Figure 14 A plot of E_A vs. pressure P for the acceptor gap in p-InSb. The line through the points is a least squares fit.

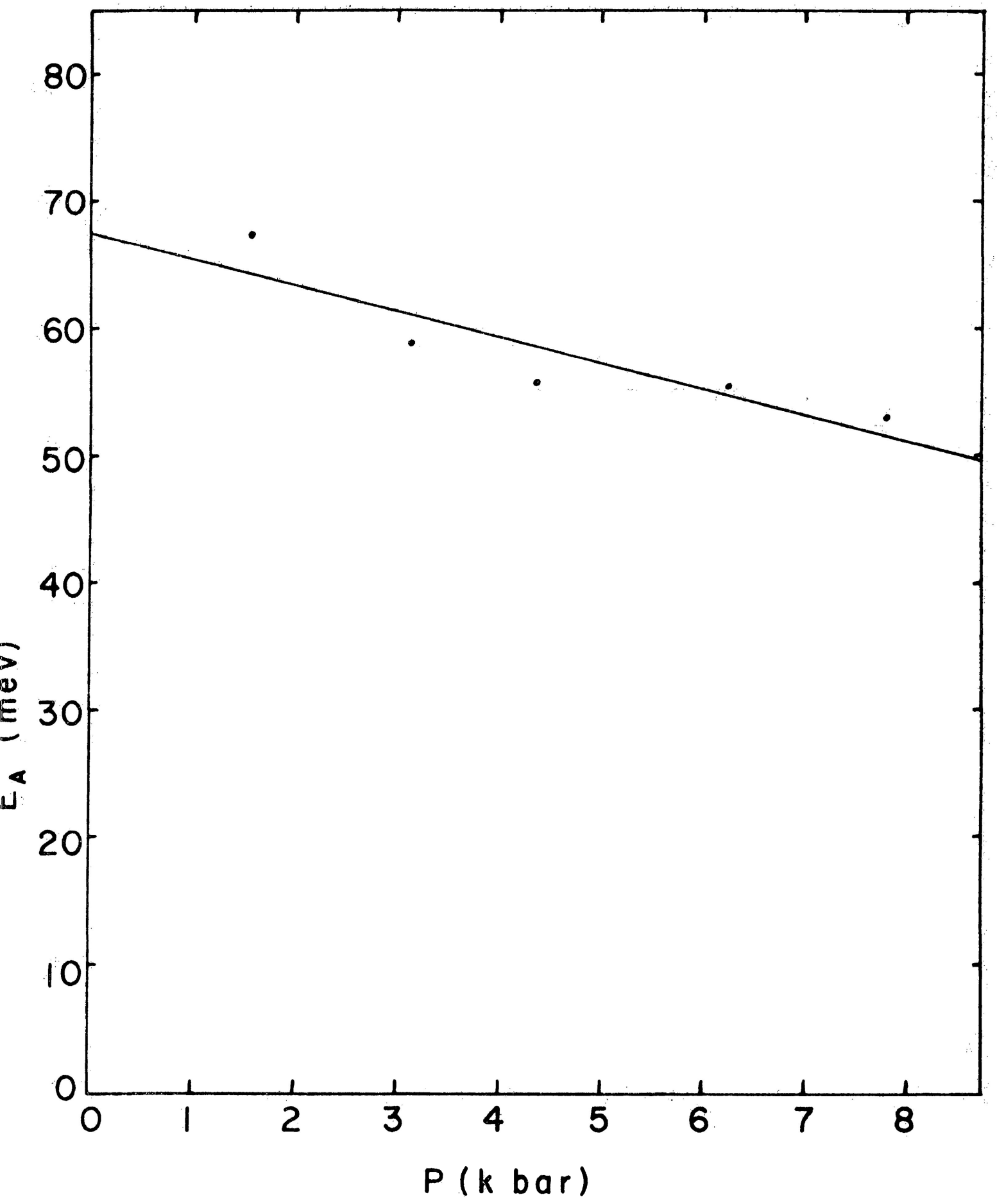
80
70
60
50
40
30
20
10
0
E_A (mev)
0
1
2
3
4
5
6
7
8
P (k bar)

$$E_{0A} = 67.4 \text{ meV}$$

$$Y_A = -2.02 \frac{\text{meV}}{\text{kbar}} \pm 1.21 \frac{\text{meV}}{\text{kbar}} \quad 90\% \text{ confidence}$$

$$\pm 2.62 \frac{\text{meV}}{\text{kbar}} \quad 99\% \text{ confidence}$$

Other workers in the field have observed an acceptor gap in p-type InSb of[37]

$$E_{0A} = 0.12 \text{ eV} \quad \lambda_A = +1 \frac{\text{meV}}{\text{kbar}}$$

This is nearly twice our value and the pressure derivative lies outside our 99% confidence interval, so it appears that a difference type of acceptor is probably involved. The significance of these results is that the acceptor levels observed in InSb have small pressure derivatives, that is they are nearly fixed in energy relative to the valence band. This bears out our assumption in section 3-2 that the hypothetical acceptor level has the same pressure derivative as the band gap.

3-4. Temperature and Electric Field Dependent Mobility and Carrier Number

I. Temperature Dependence

Temperature dependent mobility measurements made by S.M. Fong at various pressures are shown in Fig. 15.[26] In cases where freeze-out was not apparent the mobility had a temperature dependence of $T^{-1.7}$ in the temperature range 80-300^{o}K, and a dependence of $T^{0.8}$ at temperatures from 50^{o}K down. The high temperature mobility was satisfactorily explained on the basis of polar optical and electron hole scattering.

At low temperatures the scattering was assumed to be caused by impurities, and the ionized and neutral scattering limits were calculated using Eqs. (1-3-1) and (1-3-3). The number of ionized impurities was taken as the measured carrier number, and the total impurity concentration as the carrier number at zero pressure and 77^{o}K. The calculations for zero pressure yielded mobilities with the correct temperature dependence but were larger than the experimental results by a constant factor. We have since observed that this discrepancy can be removed by noting that the impurity numbers used in the calculations were taken from measured values of carrier numbers, which will be smaller than the actual number by Y_H, the Hall factor. The mobilities were recalculated, taking

$$Y_H = \sqrt{Y_{Hi}\, Y_{Hn}} = 1.4 \quad ,$$

Figure 15 A log-log plot of Hall mobility μ vs. T for n-InSb sample #1 at various pressures.

- ● P = 0 kbar
- ■ P = 4.2 kbar
- ▲ P = 8.2 kbar
- ○ P = 10.3 kbar

X represents a theoretical fit to the zero pressure curve.

Vertical bars on the two lower curves represent the range of mobility variation with electric field.

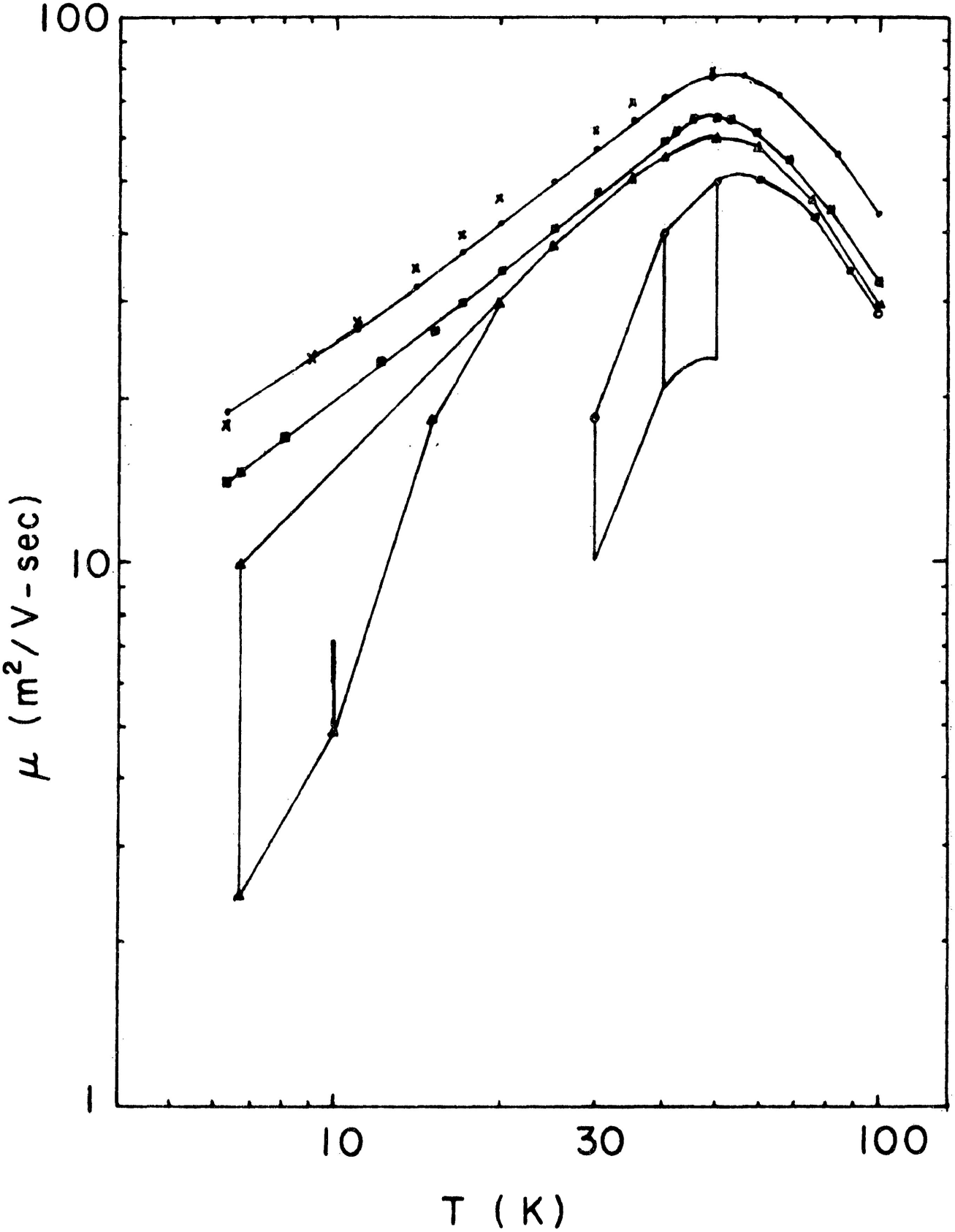
100
10
1
μ (m²/V-sec)
10
30
100
T (K)

the average of the Hall factors for ionized and neutral scattering, as these were roughly equal in importance. The results give very close agreement with the experimental values, and are also shown in Fig. 15. Increasing pressure from zero increases the electron effective mass and lowers the absolute mobility values while maintaining the same slope.

At higher pressures freeze-out occurs and the mobility is observed to drop sharply. This contradicts Porowski's statement that the scattering processes become less effective during freeze-out. The mobility values are also strongly dependent on the electric field strength, as denoted by the bars on the two high pressure curves in Fig. 15. The mobility was generally higher at low field strength.

II. Electric Field Dependence

In order to gain an understanding of mobility limiting processes in the freeze-out regime, we performed systematic studies of the field dependence of the mobility at low temperature and at various pressures both below and above freeze-out. The mobilities and carrier numbers are shown in Figs. 16a, 16b, 17 and 18 . At low pressures where freeze-out is not observed (Figs. 16a and 16b) the mobility is constant with field at low field strengths and then increases with approximately an $E^{0.33}$ dependence. This is somewhat higher than the $E^{0.25}$ dependence predicted by Stokoe

and Cornwell,[19] but their calculations are for a higher temperature of 20°K. The low field values of the mobility show the $T^{3/2}$ temperature and $m_e^{*1/2}$ pressure dependence predicted by Eq. (1-3-1) for ionized impurity scattering.

The carrier number at low pressures appears to undergo a sharp decrease at low field strengths. A similar effect was noted in temperature dependent carrier number measurements (Figs. 7 and 8) at pressures too low to cause a positive donor gap. The explanation of this phenomenon seems to be that the electrons are 'pooling' due to increasing degeneracy in the bottom of the conduction band. Electrons below the Fermi level have few neighbouring energy states to move into and thus contribute less to conduction. We calculated that the Fermi level for temperatures near 0°K for our sample should lie 0.74 meV above the conduction band minimum. The thermal energy $k_B T$ approximates this value for temperatures of the order of 10°K which is where the effect is observed, thus degeneracy would be expected. Raising the temperature or applying a high electric field will raise the electron energy, destroying the degeneracy.

At 9 kbar (Figs. 16a and 16b) there is some freeze-out and the carrier number increases approximately exponentially with electric field due to impact ionization. C. Dick and B. Ancker-Johnson[31] predict that the rate of carrier generation by impact ionization should be exponential with carrier drift velocity

$$g(E) \propto \exp(V_d/\theta) \ . \qquad (3\text{-}4\text{-}1)$$

θ is a constant. We know that $V_d = \mu E$ so that for constant mobility we should have an exponential increase in the carrier number with field strength, as observed.

The field dependence of the mobility at 9 kbar is difficult to interpret. The increasing number of ionized impurities reduces the mobility up to a point before a runaway increase sets in. This is similar to the result observed by E.M. Conwell[17] for ionized impurity scattering in germanium.

We went to higher pressures to see if another scattering mechanism became dominant when freeze-out reduced the number of ionized impurities sufficiently. The results are shown in Figs. 17 and 18. The rate of carrier generation no longer appears exponential with E because of the rapidly varying mobility. It can be seen that the field dependence of the mobility almost exactly reciprocates the carrier number and hence the ionized impurity concentration. This furnishes strong evidence to suggest that ionized impurity scattering limits the mobility even in conditions of advanced freeze-out. Other possible scattering mechanisms were considered. Neutral impurity scattering is favoured when freeze-out neutralizes a large proportion of the impurities. As noted in section 1-3 the only field dependence of this scattering process is in the number of neutral impurities which may be reduced by impact ionization. This effect should increase the mobility, whereas we observe the mobility decreasing with field, and in any case the

relative change in the neutral impurity concentration is less than 1 percent in all the high pressure runs, so the mobility limit from this process should stay nearly constant with field.

Acoustic phonon scattering is usually considered to be a high temperature effect but it can become dominant if the electron temperature is raised by an electric field. As noted in section 1-3 acoustic scattering exhibits a characteristic $E^{-\frac{1}{2}}$ field dependence which is not observed in any of our results.

Polar optical phonon scattering for low lattice temperatures can limit the electron drift velocity to a nearly constant value for a range of field strengths, producing a mobility field dependence of E^{-1}. This might account for the results in Fig. 17 but not Fig. 18. Since phonon scattering processes are not affected by impurity concentrations there is no reason why a phonon mobility limit should give the close agreement between mobility and ionized impurity number observed in all the high pressure results. We concluded, therefore, that under high pressure, ionized impurity scattering is the dominant scattering mechanism at low temperatures in InSb.

III. Impact Ionization Breakdown

The electric field was increased to breakdown at temperatures of $20^{o}K$ and $10^{o}K$ at pressures where freeze-out was advanced. The

Figure 16a Hall mobility μ vs. electric field strength E for n-InSb sample #1 at various temperatures and pressures.

● P = 0 kbar T = 11°K

X P = 0 kbar T = 6.7°K

○ P = 6.3 kbar T = 6.7°K

■ P = 9.4 kbar T = 10°K

▲ P = 9.4 kbar T = 6.2°K

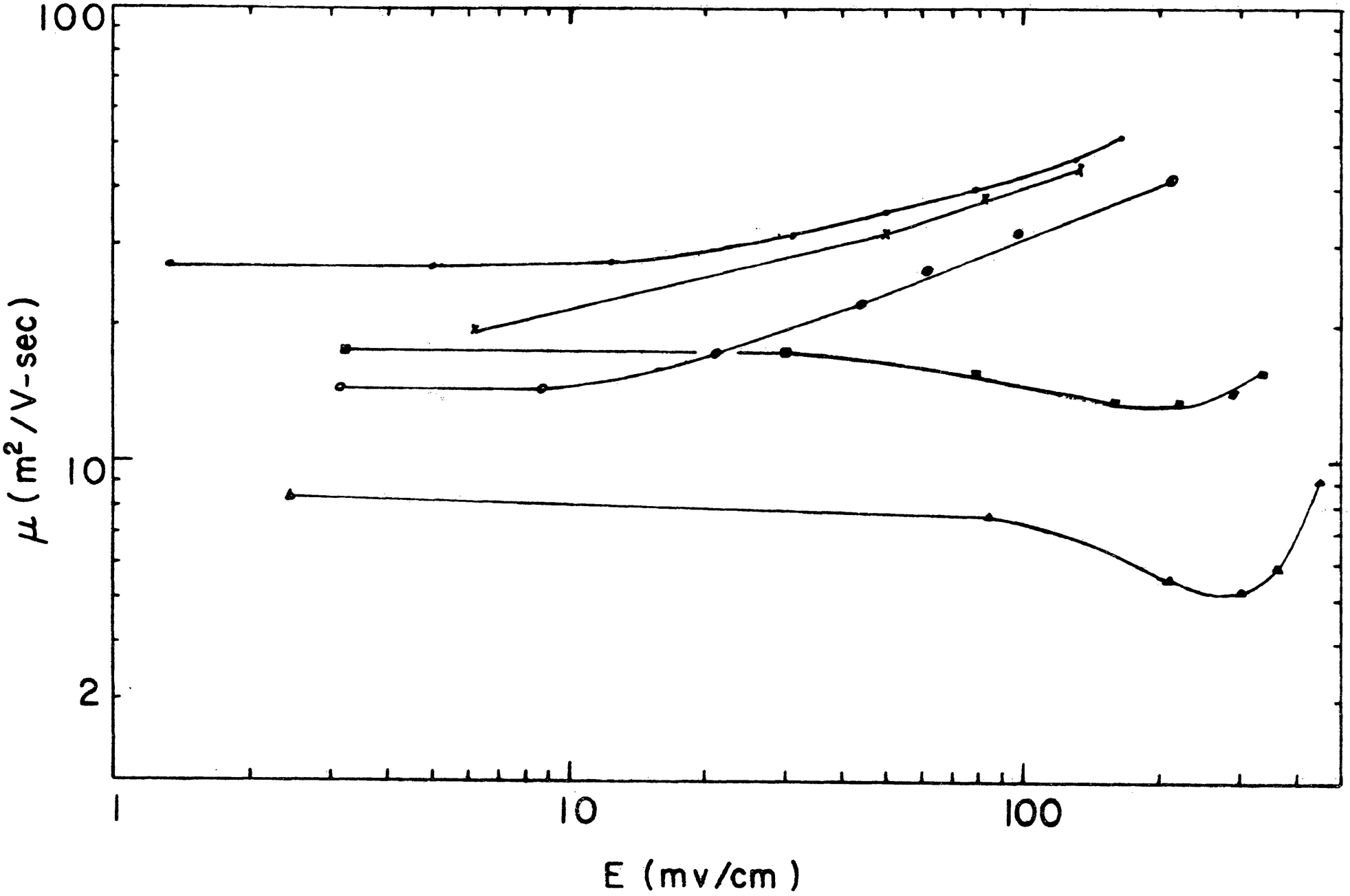
100
10
2
μ (m²/V-sec)
1
10
100
E (mv/cm)

Figure 16b A semilog plot of carrier concentration vs. electric field $\vec{E}$ for n-InSb sample #1 at various temperatures and pressures.

●	P = 0 kbar	T = 11°K
○	P = 6.3 kbar	T = 6.7°K
■	P = 9.4 kbar	T = 10°K
▲	P = 9.4 kbar	T = 6.2°K

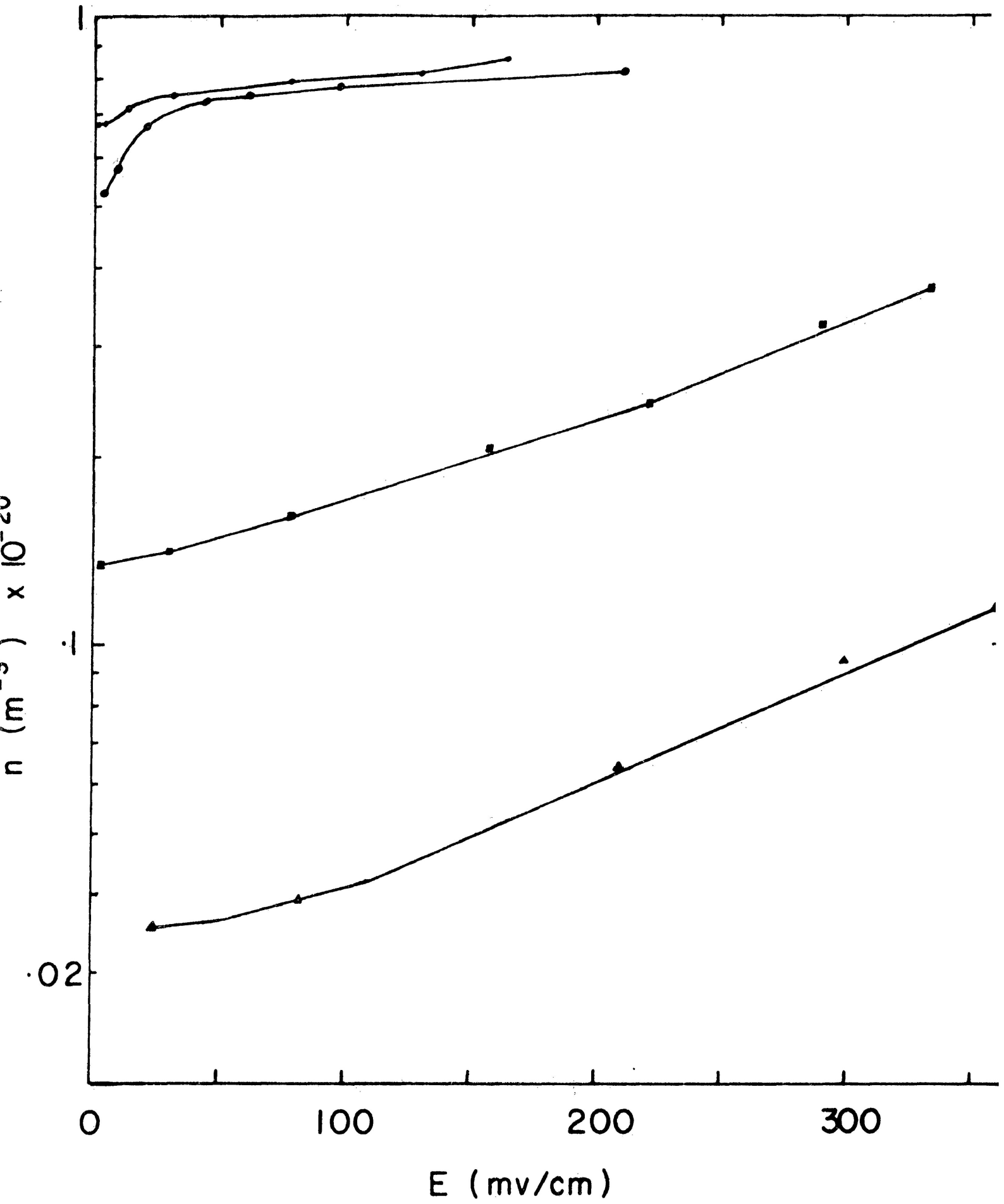
1
·1
·02
n (m⁻³) x 10⁻²⁰
0
100
200
300
E (mv/cm)

Figure 17 Hall mobility μ and carrier number n vs. electric field E for n-InSb sample #1.

● μ

■ n

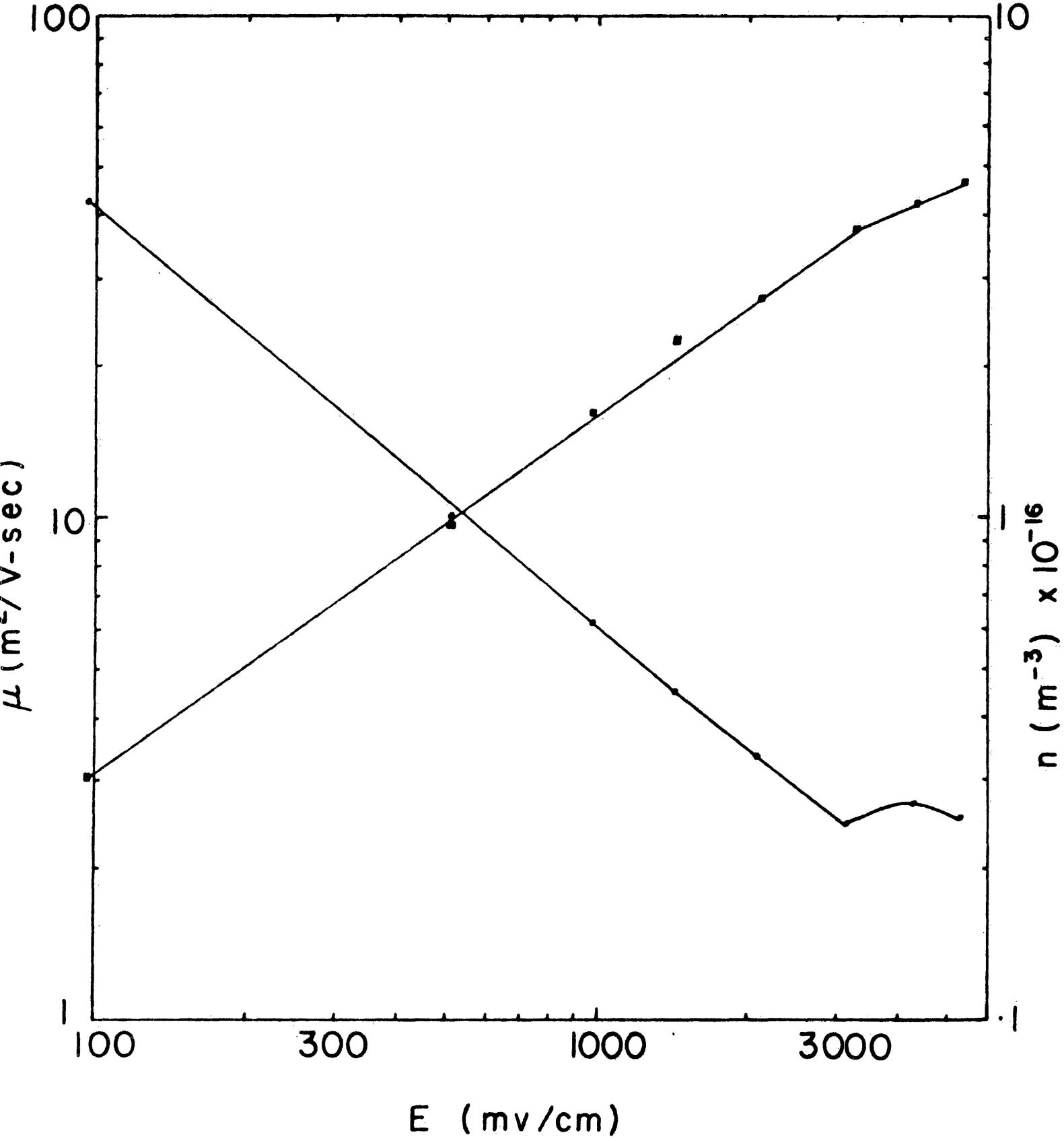
100
10
1
100
300
1000
3000
10
1
.1
μ (m²/V-sec)
n (m⁻³) x 10⁻¹⁶
E (mv/cm)

Figure 18 Hall mobility μ (upper curves) and carrier number n (lower curves) vs. electric field E at two temperatures.

- ● T = $50^{o}K$
- ■ T = $40^{o}K$

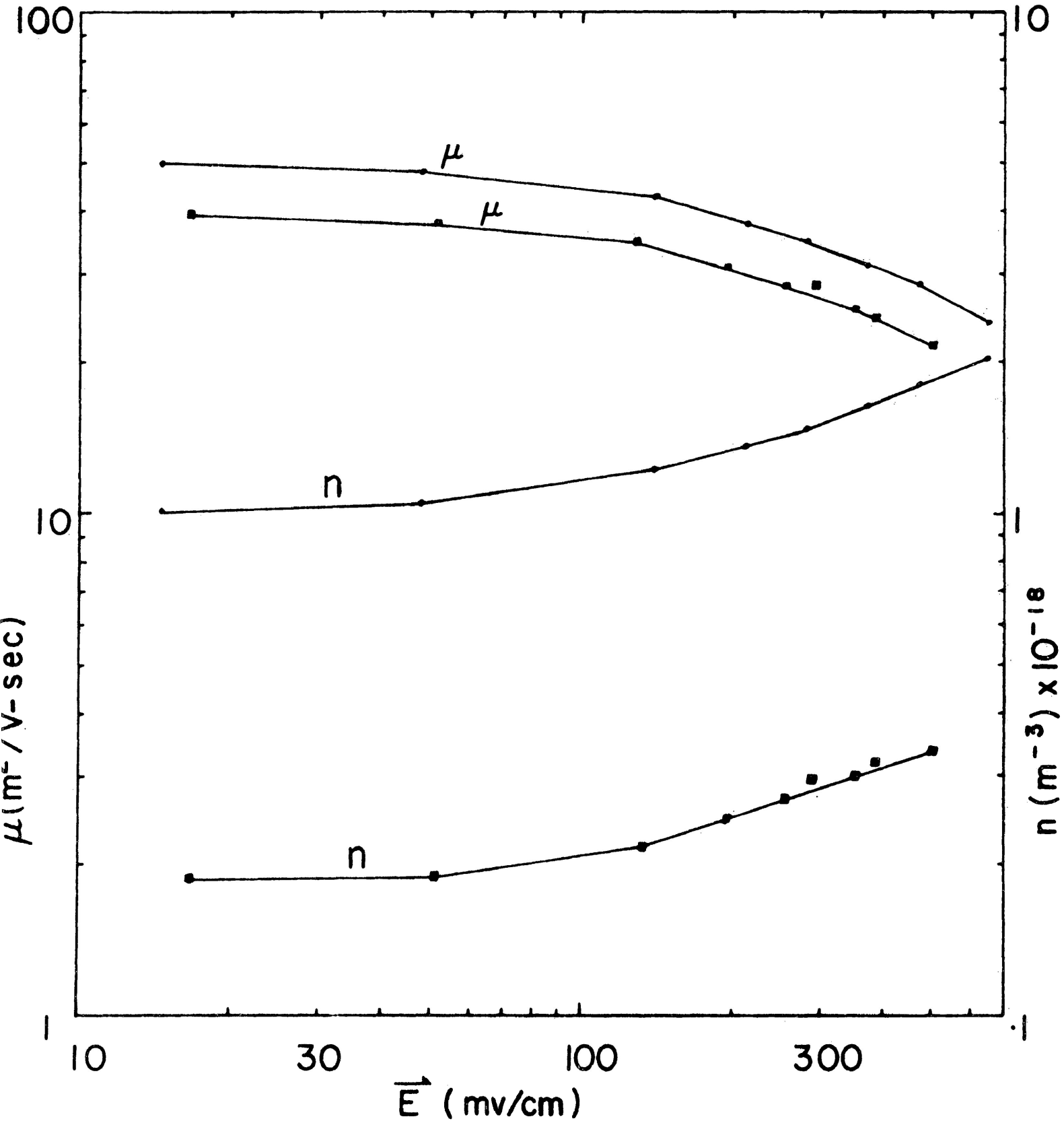
100
10
μ
μ
n
10
1
n
μ(m²/V-sec)
n (m⁻³) x 10⁻¹⁸
1
·1
10
30
100
300
E (mv/cm)

breakdown field strength lay between 10^3 and 10^4 mV/cm. It was lower at higher temperature where the mobility was higher. During breakdown the sample appeared to exhibit negative resistance properties; as the current through it was raised the electric field across it actually decreased due to the rapidly increasing carrier density. Due to this effect we were unable to determine whether there were two regions of breakdown corresponding to two donor levels.

Chapter 4

Conclusions

Donor and acceptor gap measurements have been made in n and p-type InSb as a function of pressure up to 15 kbar. Low and high field mobility measurements have been made at low temperatures and at several pressures.

The donor gaps in n-InSb are found to increase linearly with pressure, becoming zero at pressures below 8.4 kbar. The donor gap appears to change abruptly at temperatures around $100^{o}K$ as the temperature is lowered. Below $100^{o}K$ the gap appears to be approximately half as wide as the gap above $100^{o}K$. Porowski explains this by assuming that the donor ions can adopt non-equivalent lattice positions with different electron ionization energies, and the ions can transfer from one position to another across a potential barrier when the temperature is above some critical value. He shows that this will produce a different carrier freeze-out rate above and below the critical temperature. We have shown that the same effect can be produced by nearly equal concentrations of donors and acceptors. The carrier freeze-out rate above the critical temperature corresponds to an effective energy gap of the combined donor and acceptor gaps, the acceptor gap being measured from the conduction band as if it were a donor. Below the critical temperature the carrier freeze-out rate corresponds

to an effective energy gap twice the donor gap. Based on this theory we find the pressure derivatives of the assumed donor and acceptor levels (relative to the conduction band) to be close to the pressure derivatives of the L band minimum and the valence band maximum, respectively. Measurements on p-type InSb showed that the acceptor level remained essentially fixed with respect to the valence band, i.e. it had the same pressure derivative relative to the conduction band.

Mobility limiting processes at low temperature (below $40^{o}K$) in cases where carrier freeze-out is not apparent are dominated by ionized and neutral impurity scattering. When the pressure is high enough to induce carrier freeze-out the mobility is observed to decrease sharply. Investigations of the electric field dependence of the mobility at low temperature and a range of pressures indicate that ionized impurity scattering is the dominant scattering process when carrier freeze-out is advanced. Low temperature and high pressure both favor this process.

REFERENCES

1. R.J. Sladek, J. Phys. Chem. Solids, Vol. 5, p. 157 (1958).

2. R. Mansfield and I. Ahmad, J. Phys. C, Vol 3, p. 423 (1970).

3. R. Mansfield, J. Phys. C, Vol. 4, p. 2084 (1971).

4. E.W. Fenton and R.R. Haering, Phys. Rev. Vol. 159, No. 3, p. 593 (1967).

5. E.S. Itskevich and L.M. Kashuskaya, Sov. Phys. Solid State, Vol. 16, No. 10 (1975).

6. Y. Yafet, R.W. Keyes, E.N. Adams, J. Phys. Chem. Solids, Vol. 1, p. 137 (1956).

7. M. Von Orthenburg, J. Phys. Chem. Solids, Vol. 34, No. 3, p. 397 (1973).

8. A.K. Walton and J.C. Dutt, J. Phys. C, Vol. 10, p. L29 (1977).

9. E.M. Gershenzon, L.B. Litvak-Gorskaya, N.A. Serebryakova and V.B. Smirnova, Sov. Phys. Semicond. Vol. 9, No. 4, p. 440

10. E.S. Itskevich and L.M. Kashirskaya, Sov. Phys. Solid State, Vol. 16, No. 10, p. 1888 (1975).

11. E.S. Itskevich, L.M. Kashirskaya and V.A. Sukhoparov, Sov. Phys. Solid State, Vol. 16, No. 10, p. 1893 (1975).

12. S. Porowski, M. Konczykowski and J. Chrobocgek, Physics Letters, Vol. 48A, No. 3, p. 189 (1974).

13. S. Porowski, M. Konczykowski and J. Chroboczek, Phys. Stat. Sol.(a), Vol. 63, p. 291 (1974).

14. L. Dmowski, M. Konczykowski, R. Piotrykonski and S. Porowski, Phys. Stat. Sol.(b), Vol. 73, p. K131 (1976).

15. S. Porowski and L. Sosnowski, Solid State Physics Semiconductors, V. 1CHP, p. 708 (1976).

16. V.I. Kadushkin, Sov. Phys. Solid State, Vol. 16, No. 10, p. 1879 (1975).

17. E.M. Conwell, Phys. Rev. Vol. 90, No. 5, p. 769 (1953).

18. D. Matz, Phys. Rev. Vol. 189, No. 1 (1968).

19. T.Y. Stokoe and J.F. Cornwell, Phys. Stat. Sol.(b), Vol. 19, p. 651 (1972).

20. M. Tanenbaum and H.B. Briggs. Phys. Rev. Vol. 91, No. 6, p. 1561 (1953).

21. Elias Burstein, Phys. Rev. Vol. 93, p. 632 (1954).

22. E.O. Kane, J. Phys. Chem. Solids, Vol. 1, p. 249 (1957).

23. D. Long, Phys. Rev. Vol. 99, No. 2, p. 388 (1955).

24. R.W. Keyes, Phys. Rev. Vol. 99, No. 2, p. 490 (1955).

25. S. Porowski and W. Paul, Solid State Communications, Vol. 7 p. 905 (1969).

26. S.M. Fong, Lakehead University, Master's Thesis (1978) (unpublished).

27. H. Brook, Advances in Electronics and Electron Physics, Vol. 7, p. 85 (1955).

28. C. Hilsum and A.C. Rose-Innes, Semiconducting III-V Compounds, Pergamon Press, N.Y., (1961) p. 117.

29. C. Erginsoy, Phys. Rev. Vol. 79, p. 1013 (1950).

30. K. Seeger, Semiconductor Physics, Springer-Verlag (1973), pp. 179-184, 218-226.

31. C. Dick and B. Ancker-Johnson, Phys. Rev. B. Vol. 5, No. 2, P. 526 (1972).

32. Z. Dobrovolskis and A. Krotkus, Sov. Phys. Semicond. Vol. 11, No. 3, p. 324 (1977).

33. L. Van der Pauw, Philips Research Reports, Vol. 13, No. 1 (1958).

34. K.W. Keyes and R.J. Sladek, J. Phys. Chem. Solids, Vol. 1, p. 143 (1956).

35. W.S. Burnside and A.W. Panten, Theory of Equations, 3rd Edition, Longman's, London (1892) p. 28.

36. A.D. Booth, Numerical Methods, 3rd Edition, Academic Press, N.Y. (1966) pp. 162-164.

37. D.I. Aladashvili, V.V. Galavanov, L. Konizewicz, S. Porowski and L. Sosnouski, V.ICHP:1, Solid State Physics: Semiconductors, p. 688.